AFRL-AFOSR-UK-TR-2012-0043

Novel manufacturing technologies for GHz/THz integrated circuits on synthetic diamond substrates

Dr. Oleksandr Zorenko

State Enterprise Research Institute "ORION"
8-a, Ezhena Potie str.
Kyiv, Ukraine 03057

EOARD STCU 08-8007/STCU Partner Project P-368

Report Date: November 2010

Final Report from 01 November 2009 to 31 October 2010

Air Force Research Laboratory
Air Force Office of Scientific Research
European Office of Aerospace Research and Development
Unit 4515 Box 14, APO AE 09421

REPORT DOCUMENTATION PAGE

Form Approved OMB No. 0704-0188

1. REPORT DATE *(DD-MM-YYYY)*	2. REPORT TYPE	3. DATES COVERED *(From – To)*
15 November 2010	Final Report	1 November 2009 – 31 October 2010

4. TITLE AND SUBTITLE

Novel manufacturing technologies for GHz/THz integrated circuits on synthetic diamond substrates

5a. CONTRACT NUMBER

STCU Partner Project P-368

5b. GRANT NUMBER

STCU 08-8007

5c. PROGRAM ELEMENT NUMBER

61102F

6. AUTHOR(S)

Dr. Oleksandr Zorenko

5d. PROJECT NUMBER

5d. TASK NUMBER

5e. WORK UNIT NUMBER

7. PERFORMING ORGANIZATION NAME(S) AND ADDRESS(ES)

State Enterprise Research Institute "ORION"
8-a, Ezhena Potie str.
Kyiv, Ukraine 03057

8. PERFORMING ORGANIZATION REPORT NUMBER

N/A

9. SPONSORING/MONITORING AGENCY NAME(S) AND ADDRESS(ES)

EOARD
Unit 4515 BOX 14
APO AE 09421

10. SPONSOR/MONITOR'S ACRONYM(S)

AFRL/AFOSR/RSW (EOARD)

11. SPONSOR/MONITOR'S REPORT NUMBER(S)

AFRL-AFOSR-UK-TR-2012-0043

12. DISTRIBUTION/AVAILABILITY STATEMENT

Approved for public release; distribution is unlimited.

13. SUPPLEMENTARY NOTES

14. ABSTRACT

A frequency multiplier with IMPATT diode having high multiplication ratio served as a device demonstrating the advantages of diamond application as substrate. We chose output frequencies of 280 GHz and 360 GHz to perform analysis and calculations as well as for experimental studies.
Choosing of diamond substrate thickness makes a complex problem. On the one hand, one should decrease the dielectric thickness as frequency grows to reduce the transmission line width. On the other hand, in that case the transmission line losses increase. Thus, the above problem is to be considered separately for each specific application. In this project, we chose diamond thickness of 30 um for multiplier realization.
The successful development and simulation of the elements of frequency multiplier with high multiplication ratio that have satisfactory parameters indicate possibility of realization of ICs on diamond substrates.
In the course of our studies it was found that the Ti-Pd-Au metallization system (thickness of 2-3 um) can be applied when forming the topology of IC elements on synthetic diamond layers, while the Cr–Cu–Ni–Au metallization system with thick (up to 50 um) copper layer can serve as screen heat sink and HIC elements carrier.
We did not found considerable interaction processes in the Ti–Pd–Au metallization layers at temperatures up to 400 ºC. This indicates its rather high thermal stability and possibility of application in technological processes of microwelding and flux-free soldering at temperatures up to 400 ºC.
The technical documentation on fabrication of photomasks for IC topology formation in frequency multipliers with silicon IMPATT diodes with operating frequencies of 280 GHz and 360 GHz was developed.
A manufacturing scheme for IMPATT diode based on the silicon thin membrane technology was developed. The photomasks were designed and fabricated to realize the manufacturing scheme. A set of photomasks ensures formation of beam leads and mesas using the double-sided photolithography. The technological processes were refined in accordance with the manufacturing scheme.
The silicon beam-lead IMPATT diode parameters (differential resistance and capacitance) can be adjusted to the required values after diode mounting in IC.

15. SUBJECT TERMS

EOARD, Electrotechnollogy And Fluidics, Electrooptical and Optoelectronic Devices

16. SECURITY CLASSIFICATION OF:			17. LIMITATION OF ABSTRACT	18, NUMBER OF PAGES	19a. NAME OF RESPONSIBLE PERSON
a. REPORT	b. ABSTRACT	c. THIS PAGE			SCOTT DUDLEY, Lt Col, USAF
UNCLAS	UNCLAS	UNCLAS	SAR	46	19b. TELEPHONE NUMBER *(Include area code)* +44 (0)1895 616162

FINAL REPORT

NOVEL MANUFACTURING TECHNOLOGIES FOR GHZ/THZ INTEGRATED CIRCUITS ON SYNTHETIC DIAMOND SUBSTRATES

EOARD Project 088007
(STCU Partner Project P-368)

State Enterprise Research Institute "ORION"
Kyiv, Ukraine

15th November 2010

Novel manufacturing technologies for GHz/THz integrated circuits on synthetic diamond substrates

Final EOARD Report covering the period 1.11.2009 to 31.10.2010

State Enterprise Research Institute "Orion", Kyiv, Ukraine

Table of Contents

1 List of Figures

2 Summary

In view of low dielectric losses, diamond is very promising material for application at GHz and THz frequencies. Its greatest advantage is high thermal conductivity. Therefore, use of diamond substrates when manufacturing integrated circuits (ICs) will make it possible to improve considerably thermal conditions of active elements assembled in a microcircuit. Thus, one can obtain higher reliability and power output of microcircuits. In addition, such microcircuits can operate in high-temperature ambiances; this opens wide possibilities for their application.

The goal of the project was to develop novel manufacturing processes of microwave integrated circuits based on synthetic diamond substrates obtained using chemical vapor deposition.

To accomplish this goal several auxiliary tasks must have been done, such as determination of the ways of coherent signal sources development in span 100 to 1000 GHz utilizing integrated circuits on 50-200 um diamond wafers and possibilities to create new manufacturing processes for such circuits. It also included simulation of integrated circuit elements, their thermal and electrical characteristics, layout development and determination of requirements for microwave parts of integrated circuits. Production of photomasks and development of new microelectronic manufacturing processes that are necessary for the production of microwave modules prototypes on diamond substrates was done after development of integrated circuit layouts and simulation of elements.

The first step was to develop a device to demonstrate the diamond advantages. It included choosing the most appropriate device and developing layouts of its main parts. We developed topology of a frequency multiplier of high multiplication ratio on a diamond substrate and performed corresponding simulation. Just this device has been chosen because it enables one to demonstrate diamond advantages very clearly. Our work proved that development of devices on diamond substrates is possible.

We developed technological procedures for metallization systems to be used in manufacturing of topology elements for microstrip ICs. The metallization systems were studied to determine their thermal stability. The results obtained enabled us to choose such metallization systems that are most suitable for realization of THz ICs on diamond substrates. The manufacturing routes were chosen with allowance made for the diffusion processes occurring in multilayer microstrip structures in the course of flux-free welding.

We also developed a design of miniature silicon multiplier beam-lead IMPATT diode intended for assembly in the IC layout elements. To realize the manufacturing scheme

for IMPATT diodes, the photomasks were developed, designed and made. The prototypes of such diodes were made, and the test IC samples manufactured.

At the end of the project, investigations of the electrical properties of metal-diamond-metal structure were performed in wide range of voltages between the ground plane and signal board (up to 400 V) and temperatures (+20…+400°C). The IMPATT diode capacitance was adjusted to the required value (0.2 pF) by additional mesa etching, and the diode low-frequency parameters after mounting and additional etching were studied.

Thus, the goal of the project was achieved.

3 Introduction

In recent years, the development of THz facilities becomes of more importance. This is because high operating frequency makes it possible to obtain high data transfer rate in various information systems, high accuracy in navigation systems and many other advantages. Physical dimensions of THz devices are very small. This is especially important for aerospace systems. In addition, the THz devices have potentialities for application in radiometric imaging, in particular, in antiterrorist systems.

Some properties of diamond make it very promising material for application at THz frequencies. These are record-breaking values of hardness and thermal conductivity, minimal dielectric losses at the above frequencies, transparency in the range from UV to radio waves, chemical and radiation strength and high charge carrier mobility [1-8].

To prepare diamond layers with thickness up to 1.5 mm, the chemical vapor deposition (CVD) technique is applied, with use of microwave plasma to decompose reagents [8-10]. The most important advantages of CVD-grown films are large areas, high reproducibility of their physical parameters owing to possibility of thorough control of growth conditions and purity of the gases used and possibility to grow products of preset form [12].

Thermal conductivity and low dielectric losses in hybrid ICs (HICs) are the governing factors that have to be taken into account to ensure reliable operation of devices and their high electric characteristics. The most appropriate for high-power GHz and THz ICs are substrates of synthetic CVD-grown diamond. Their thermal conductivity may be as high as 1800–2000 W/mK [13], while the dielectric loss tangent $\tan\delta$ may be less than 10^{-5} at 100–200 GHz frequencies [14]. The existing technologies of diamond films growing on silicon substrates agree well with the manufacturing routes of microwave semiconductor technologies.

The diamond advantages can be presented more completely using a frequency multiplier with high multiplication ratio made with a silicon impact avalanche and transit-time (IMPATT) diode. One of the problems that appear when developing such devices is how to ensure a good diode heat sink. High thermal conductivity of diamond makes it possible to realize efficient heat removal, thus increasing power output at THz frequencies. This advantage becomes even more important when using IMPATT diodes made of a wide-gap semiconductor material (say, SiC). The SiC IMPATT diodes have higher efficiency than the silicon ones and can operate at much higher temperatures.

The development of frequency multiplier on a diamond substrate involves two stages. One of them is the development of topologies of multiplier and its elements as well as their electromagnetic and thermal simulation. Another stage is the development of technological processes for realization of the topologies developed and fabrication of device prototypes.

In the course of the first quarter of the project realization, we developed topologies of some multiplier elements as well as performed their electromagnetic simulation and estimation of their characteristics. We also developed the tentative topology of the multiplier as a whole.

Concurrently we also developed the manufacturing technology for metallization systems to be used in topology elements of microstrip ICs based on the Ti (0.05 μm)–Au (0.2 μm) and Ti (0.05 μm)–Pd (0.05 μm)–Au (0.1 μm)–Au (2–3 μm) metallizations.

In the second quarter of the project, we made photomasks to form layout of ICs on diamond substrates. The technological processes were refined, and technological conditions of microstrip elements and grounding layer formation according to the process flow for IC fabrication (that have been developed in the first quarter) were optimized.

The layout of the microwave frequency multiplier IC that has been developed in the first quarter involves application of a miniature silicon multiplier IMPATT diode with beam leads. Therefore, it was necessary to develop and make laboratory patterns of such diodes.

In the third quarter of the project, we refined the manufacturing technology for prototypes of multiplier IC chips on diamond substrate (operation frequency of 280 GHz). The IC was a 4×1 mm diamond board 30 μm thick, of high-ratio multiplier layout, with microstrip transmission lines. A miniature beam-lead IMPATT diode was mounted in that IC. To ensure mechanical strength of the chip and its reliable mounting in the IC package, the ground plane (and heat sink) of the microstrip line thickness was about 50 μm.

Since the layout of microwave IC multiplier involved application of an ultra-miniature silicon multiplier beam-lead IMPATT diode, it was necessary to make laboratory models of the beam-lead IMPATT diodes and diamond microstrip board.

We developed the corresponding flow charts and made the boards and silicon beam-lead IMPATT diodes (the beam lead width was 50 μm, i.e., such as that of the microstrip transmission line) as well as performed refinement of the technological processes used in mounting beam-lead IMPATT diode in the multiplier IC chip, with following correction of IMPATT diode capacitance value by additional etching of the silicon mesa.

The main problem that was dealt with at the fourth stage was the necessity of accurate adjustment of diode impedance with the other multiplier elements. To this end, the diode capacitance should be about 0.2 pF. This value could be achieved if the diode diameter is less than its thickness. This may complicate considerably the mounting process because the diode with the above interrelation between its sizes may be damaged in the course of its welding to microstrip line using thermal compression.

To make the diode mounting in IC easier, we decided to prepare diodes of bigger diameter and after their welding decrease the diode diameter using etching.

4 Methods, Assumptions, and Procedures

4.1 CVD growth of diamond

The diamond layers used in the project were grown on the 13×13 mm Si (100) substrates in a microwave discharge at a УПСА-100 plant (microwave power up to 5 kW, frequency of 2.45 GHz). The reaction mixture CH_4 (3%)/H_2 (97%) was used according to procedure similar to that described in [9-15]. The deposition conditions were as follows. Hydrogen flow discharge was 0.66 l/min., chamber pressure of 85 Torr, microwave power input of 3.2 kW, substrate temperature of 940 ºC. The diamond films thicknesses were 15–45 μm, the growth rate was 10–1.8 μm/hour.

The Raman spectra of films had the only peak at 1332 cm^{-1}. This fact indicated the purely diamond structure of the samples obtained. X-ray diffraction (XRD) analysis showed that the synthetic diamond layers grown on single-crystalline silicon had fine-crystalline structure. The character of XRD spectra and unit cell parameters showed that there were no considerable intrinsic stresses in the sample. We also did not detect graphite phase traces in the synthetic diamond layers. Thus, the XRD data confirmed the conclusions of Raman spectroscopy that the initial diamond layers had a high-quality fine-crystalline structure, without considerable micro- and macroscopic stresses.

4.2 Electromagnetic calculations and simulation

In our analytical calculations of the parameters of transmission lines on diamond substrates, we used the classic expressions for microstrip lines [16, 17]. When analytical calculation would be complicated or inaccurate, we applied numerical simulation with finite element method in the Ansoft HFSS environment. In such a way, in particular, we estimated transmission line losses as well as developed topologies of IC elements.

4.3 Technological processes

The Ti and Pd layers were formed with vacuum deposition, while a gold layer was prepared by combining vacuum deposition (0.1–0.2 μm) and electrochemical deposition (2–3 μm). Taking into account that the diamond layer thickness should lie in the 15–45 μm range, a transmission line ground plane has to serve as efficient heat sink as well as provide mechanical strength of synthetic diamond wafer and diamond microwave HICs packaging. To this end, we chose a Cr (0.05 μm)–Cu (0.5–1 μm)–Cu (30–50 μm)–Ni (1–2 μm)–Au (2–3 μm) metallization system. The first two metallization layers (chromium and copper) were prepared using vacuum deposition while the rest were made with the electrochemical deposition technique.

The technological procedures of layer deposition in the vacuum were refined on using upgraded commercial УВН-60М sputtering plants with oil-free turbo-molecular pumps. The pressure in the operating plants was 10^{-6} mm Hg. When sputtering Cr, Pd and Cu, we used directional evaporators made of single-crystalline molybdenum. The evaporators were heated up to the required temperature using a ring electron-beam evaporator from a cooled copper crucible. The layer parameters were monitored in the

course of sputtering from surface conductivity using the special test structures. Sputtering was made onto the diamond substrate whose temperature was 400 °C.

At this stage of project execution, we chose the manufacturing routes taking into account those diffusion processes in multilayer microstrip structures that occurs at flux-free welding. After studying the requirements on thicknesses and types of coatings, we developed the manufacturing route for microwave HICs topology as well as the whole complex of corresponding technological procedures.

Thermal stability of metallization system elements in the Ti–Au and Ti–Pd–Au metallization systems was studied using Auger electron spectroscopy with layer-by-layer analysis of system composition. The samples were studied both in the initial state (after layer deposition) and after thermal treatments at a temperature of 400 °C that imitated microwelding processes. We determined elemental composition of the sputtered layers and content of uncontrolled contaminants that accompany the vacuum sputtering process. These are, first of all, oxygen and carbon. To ensure efficient control of elemental composition over the whole system thickness, 0.05–0.1 μm metal layers were formed.

Diamond surface morphology was studied with an atomic force microscope NanoScop IIIa (DJ).

4.4 Choice of device to demonstrate the technology advantages

It was noted above that the main advantage of diamond is its high thermal conductivity. Owing to this fact, it is possible to implement high-power sources of microwave radiation at GHz/THz frequencies made as ICs. This advantage can be presented more clearly using a frequency multiplier with high multiplication ratio made with a silicon IMPATT diode. One of the problems that appear when developing such devices is provision of good diode heat sink. High thermal conductivity of diamond will ensure realization of an efficient heat sink, thus increasing power output at THz frequencies. This advantage becomes even more important when using IMPATT diode made of a wide-gap material (e.g., SiC). The SiC IMPATT diodes have higher efficiency than the silicon ones, and their power output is an order of magnitude higher than that of silicon IMPATT diodes. In addition the SiC IMPATT diodes can operate at much higher temperatures.

In this project we developed as an example frequency multipliers with multiplication ratios of 7 and 9 (from 40 GHz to 280 GHz and 360 GHz).

4.5 IMPATT diode

According to the preliminary calculations [18], the structure of IMPATT diode intended for assembly in IC with operating frequency within 280–360 GHz has to be of p^+-n-n^+-type, with space-charge region thickness no more than 0.5 μm, the majority charge carrier concentration of $(3\div5)\times10^{17}$ cm^{-3}, and have the lowest series loss resistance. The diode capacitance has to be no more than 0.15 pF. Such parameters can be realized for diodes with beam leads. At the same time, such a design can be conveniently and reliably mounted on a diamond substrate.

A design-technological simulation was performed for a frequency multiplier IMPATT diode. From its results, the diode design was developed (see Fig. 1).

The diode developed is a mesa of n^{++}-n^{+}-n-p^{+}-p^{++}-type with gold beam leads. The initial mesa diameter is 40 μm; the beam lead thickness is 6 μm. We reduced the mesa diameter to 12÷15 μm by successive etching after diode assembly on the IC chip.

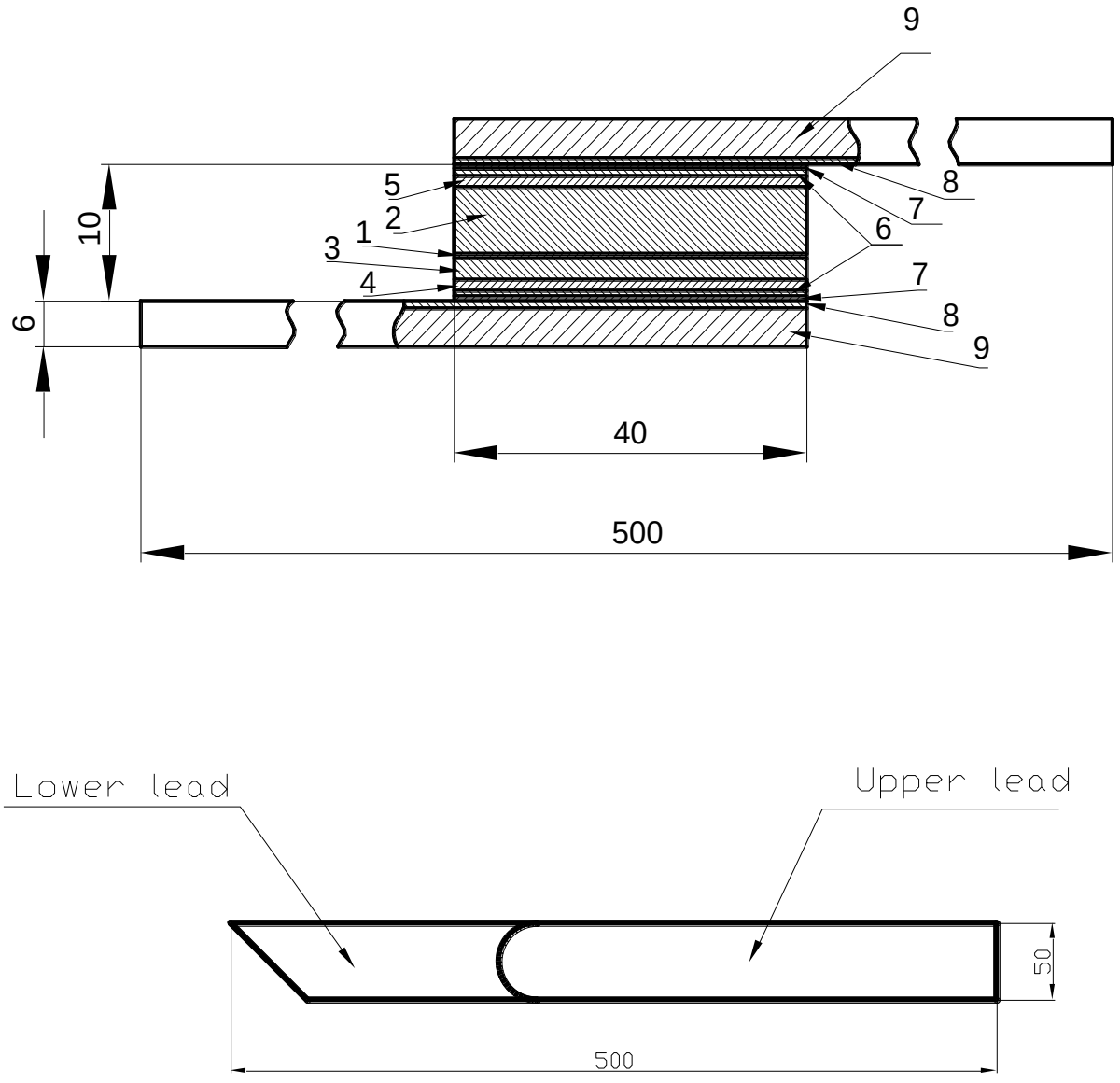

Figure 1. Design of unpackaged IMPATT diode with beam leads.
(**1** – n-layer (diode active area); **2** - n^{+}-substrate; **3** - p^{+}-layer; **4** - p^{++}-layer; **5** - n^{++}-layer; **6,7** - Pd_2Si, Ti ohmic contacts; **8, 9** – deposited and grown Au layers (beam leads)). The sizes are given in microns.

4.6 IMPATT diode mounting in IC

When mounting a IMPATT diode in IC chip, the diode was placed in such a way as to make possible welding of the lower contact and mesa to microstrip and ensure good heat transfer from mesa to the diamond substrate (Fig. 2). The upper contact beam lead should ensure electric connections to the microstrip with minimal inductance value.

4.7 Measurement of electrical parameters and characteristics of metal-diamond-metal structure

Along with the transmission lines, a round test element (diameter of 100 μm) was formed on the prototypes to investigate the electrical characteristics of the diamond layer. The test element was a capacitor with diamond insulator (metal-diamond-meta). We measured *I-V* and *C-V* curves of the metal-diamond-metal structure as well as their temperature dependences (up to 400°C). The test voltage was as high as 400 V.

Figure 3 presents a photograph of the stand used to measure the *I-V* and *C-V* curves of the structures studied in the +20 ÷ +400°C temperature range.

4.8 Measurement of mechanical parameters of metal-diamond-metal structure

The adhesion between the transmission lines and the substrate was investigated with a tester 12МП5/20-1 for mechanical studies using measurements of force required to break off the contact pad from the substrate (Fig. 4). A 4-5 mm gold wire (50 μm in diameter) was welded to the test pad using thermal compression. The value of force per unit area at which break-off occurs at the site of gold wire bonding to the test pad was determined with the tester.

4.9 Adjustment of IMPATT diode impedance

After IMPATT diode mounting in IC, its capacitance should be reduced by decreasing the silicon mesa diameter. This is achieved by using chemical etching of the mesa of IMPATT diode mounted in IC chip with further bringing its capacitance to a value below 0.2 pF.

It is impossible to control the capacitance of IMPATT diode mounted in IC chip because of big capacitance of transmission line elements. Therefore, the control of diameter (and capacitance) of the IMPATT diode mounted in chip of multiplier IC on diamond substrate was performed from its differential resistance (at a fixed value of forward current) that depends on the mesa diameter.

4.10 Characterization of IMPATT diodes

The IMPATT diode characterization was performed with the characteristic meter ЛІ2-56 and digital meter LCR E7-12 using a probe instrument.

The initial measurements were made for diodes mounted in a standard microwave package intended for mm waves. In the course of silicon mesa etching, the capacitance was measured after each step of etching.

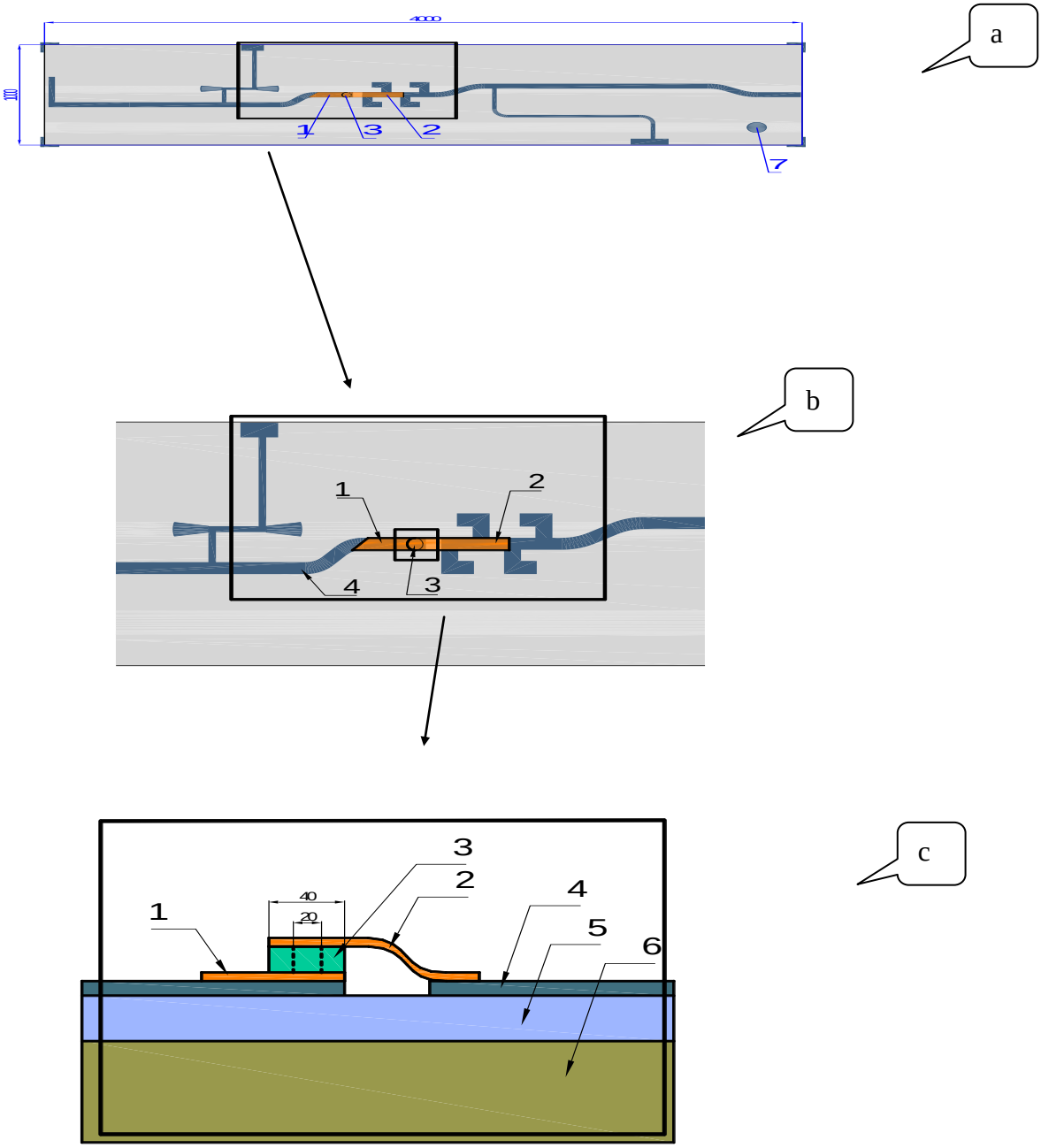

Figure 2. Layout of 280 GHz frequency multiplier with a mounted beam-lead IMPATT diode

a – fragment of multiplier layout (top view), b – enlarged fragment of multiplier layout at the diode mounting site (top view), c – enlarged fragment of multiplier layout at the diode mounting site (side view). 1 – lower lead of IMPATT diode, 2 – upper lead of IMPATT diode, 3 – silicon mesa, 4 – gold microstrip transmission line, 5 – diamond substrate, 6 – gilded copper heat sink, 7 – test metal-diamond-metal structure. (The sizes are given in microns.)

Figure 3. Photograph of the stand for characterization of metal-diamond-metal structure in the 25÷400°C temperature range

1 – high-temperature stage, 2 – binocular microscope МБС-2, 3 – device Л2-56 to take *I-V* curves, 4 – device Е7-12 to measure *C-V* curves, 5 – microstrip board on diamond substrate.

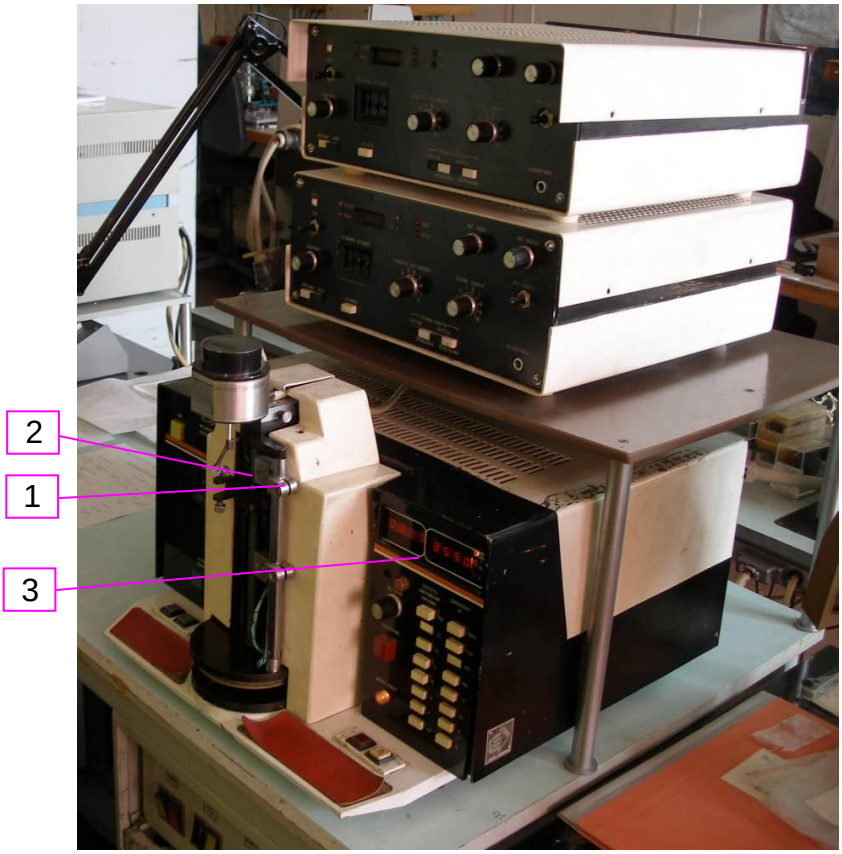

Figure 4. Setup for investigation of contact system-synthetic diamond adhesion using break-off technique – a tester 12МП5/20-1 for mechanical studies

1 – microstrip board with welded gold wire 50 μm in diameter, 2 – mechanism for smooth force increase, 3 – digital force indicator and break-off indicator.

5 Results and Discussion

5.1 Parameters of transmission lines

One of the most widespread and simple transmission lines used in microwave ICs are microstrip lines. Just this type of transmission lines is applied to make practically all multiplier elements. That is why the first step in designing its topology is the choice of construction parameters of a microstrip transmission line and estimation of its characteristics for the chosen parameters.

One of the decisive factors when choosing the parameters of a transmission line at GHz/THz frequencies is the value of line losses. The biggest contribution to the losses of transmission lines on diamond substrates comes from losses in a conductor [22]. Owing to rather high diamond permittivity (ε = 5.7), the electric field in transmission lines on such a substrate propagates predominantly through an insulator, and radiation losses are insignificant. Because of very small dielectric loss tangent ($\tan\delta < 10^{-5}$), dielectric losses are low too. The losses in conductor are due to several factors, among which are metal conductivity of the grounded layer and conductors, skin effect and surface roughness.

At a fixed value of line impedance, the losses in conductor grow as the substrate thickness decreases, because in this case, the transmission line width decreases and, correspondingly, its resistance increases. Figure 5 shows long attenuation in a microstrip line on a diamond substrate as function of line width (at several values of substrate thickness).

On the other hand, the wavelength in diamond (λ_0) is small at THz frequencies. To illustrate, $\lambda_0/4$ is about 100 μm at a frequency of 0.36 THz. If the transmission line width and wavelength at operating frequency in it are close, then making design of IC elements becomes complicated and IC parameters go down. Therefore, it seems reasonable to decrease the line width bearing in mind ease of development of THz IC elements topology. One can do this by reducing the substrate thickness only.

Let us choose the substrate thickness to be 30 μm. By applying the corresponding equations from [17], one can determine easily that the width of a 50 Ω microstrip line on diamond substrates of the chosen thickness is 47 μm. This is approximately equal to $\lambda_0/8$ at a frequency of 360 GHz and $\lambda_0/12$ at a frequency of 280 GHz. The losses in a line with impedance of 50 Ω are about 0.4 dB/mm at the above thickness of dielectric.

5.2 Electromagnetic simulation, topology

To implement a frequency multiplier whose equivalent circuits at different frequencies are presented in Fig. 6, it is necessary to develop the following elements:

- filters for supply of diode bias voltage;
- rejection filters for frequencies 280 GHz and 360 GHz;
- transition from a microstrip line to rectangular waveguide for frequencies 280 GHz and 360 GHz.

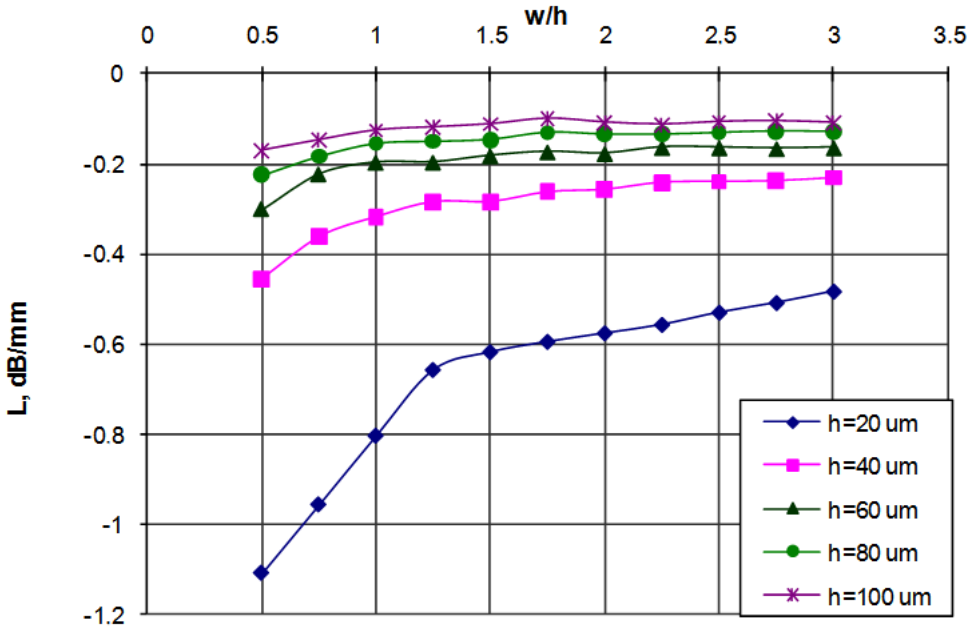

Figure 5. Long attenuation vs microstrip line width at different diamond substrate thicknesses.

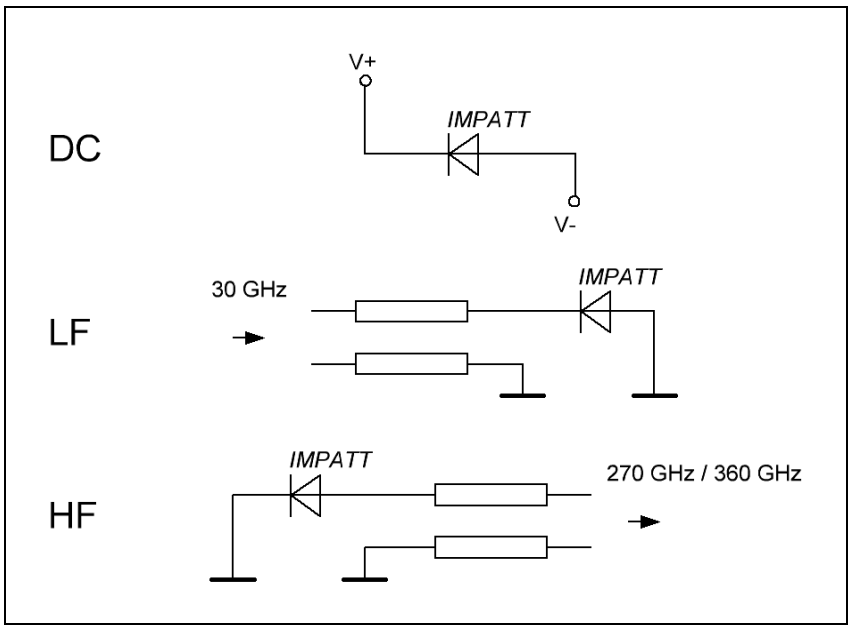

Figure 6. Multiplier equivalent circuits at different frequencies.

5.2.1 Filter for supply of diode bias voltage

The requirements for a filter for supply of diode bias voltage are as follows:

- to supply bias voltage (U_{bias}) to the active element;
- to transmit a microwave signal from input (RF In) to output (RF Out) with minimal losses.

Figure 7 shows topology of such a filter. This filter is to be set after the active element (IMPATT diode). Thus, it has to introduce minimal losses at frequencies of 280 or 360 GHz. The sizes of elements for the chosen frequencies were obtained with HFSS. Shown in Figs. 8 and 9 are the transmission (S_{21}) and reflection (S_{11}) coefficients for the topologies developed that were obtained with simulation.

Since the metallization layer in such a topology is continuous, supply of direct voltage or a low-frequency modulation signal from the U_{bias} input is made automatically. Another necessary condition is fulfilled too. An analysis showed that losses in such filters do not exceed 0.42 dB and 0.32 dB at frequencies of 280 and 360 GHz, respectively.

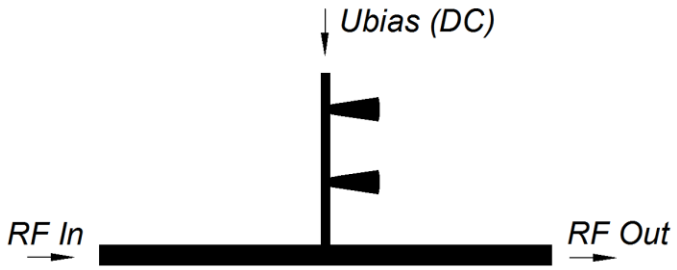

Figure 7. Topology of a filter for supply of diode bias voltage U_{bias}.

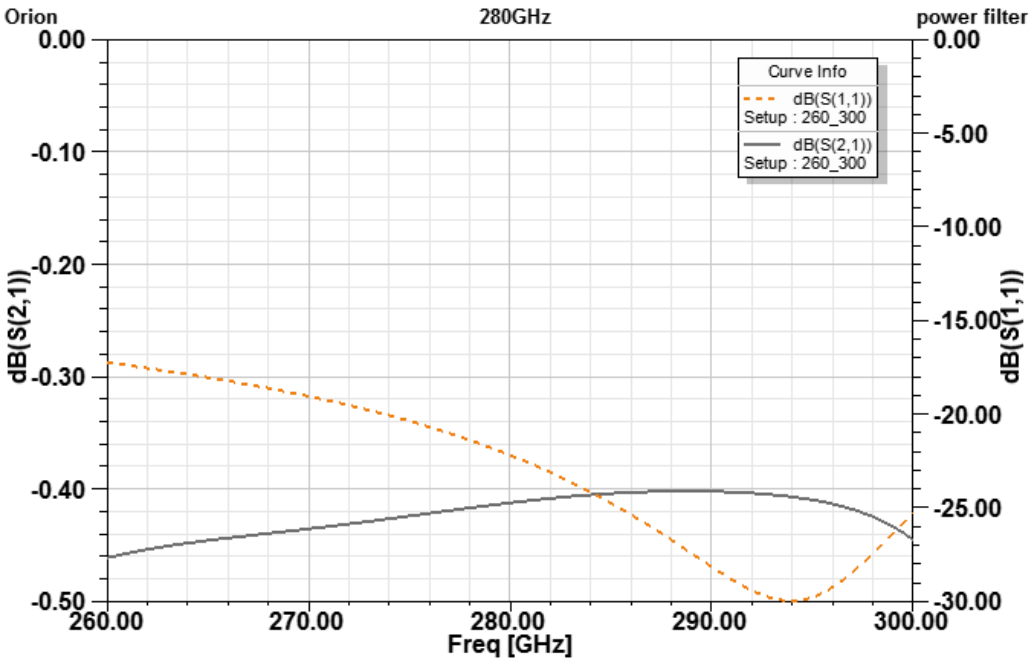

Figure 8. Transmission (S_{21}) and reflection (S_{11}) coefficients of a filter for supply of diode bias voltage at a frequency of 280 GHz obtained with HFSS.

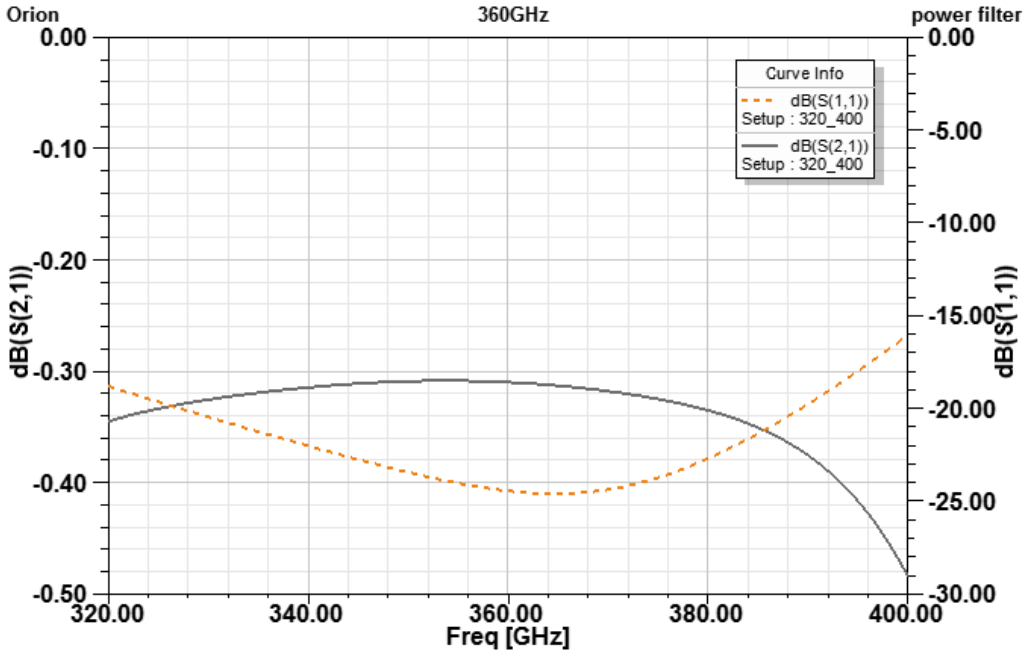

Figure 9. Transmission (S_{21}) and reflection (S_{11}) coefficients of a filter for supply of diode bias voltage at a frequency of 360 GHz obtained with HFSS.

5.2.2 Rejection filter

Figure 10 presents the rejection filter topology. This filter is intended for isolation of an active element from the IC input at high frequency. In addition, the rejection filter must transmit the master frequency with minimal losses. The sizes of the elements of that filter for the frequencies 280 GHz and 360 GHz were obtained with HFSS. Shown in Figs. 11 and 12 are the transmission (S_{21}) and reflection (S_{11}) coefficients for the topologies developed. One can see that such a filter introduces attenuation over 50 dB at the multiplier output frequency. At the same time, the introduced losses at the reference generator frequency (40 GHz) do not exceed 0.5 dB in both cases.

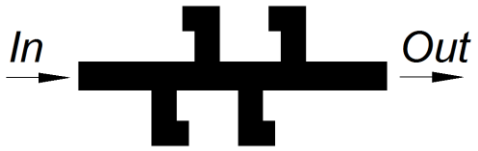

Figure 10. Rejection filter topology.

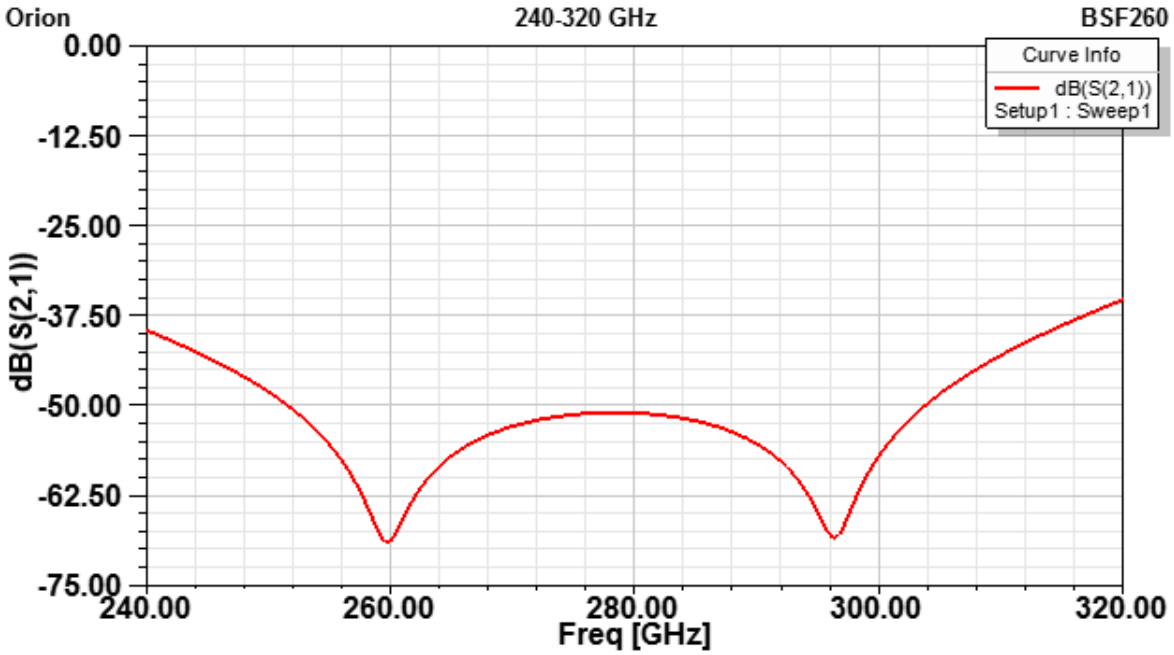

Figure 11. Transmission (S_{21}) and reflection (S_{11}) coefficients of a rejection filter at a frequency of 280 GHz obtained with HFSS.

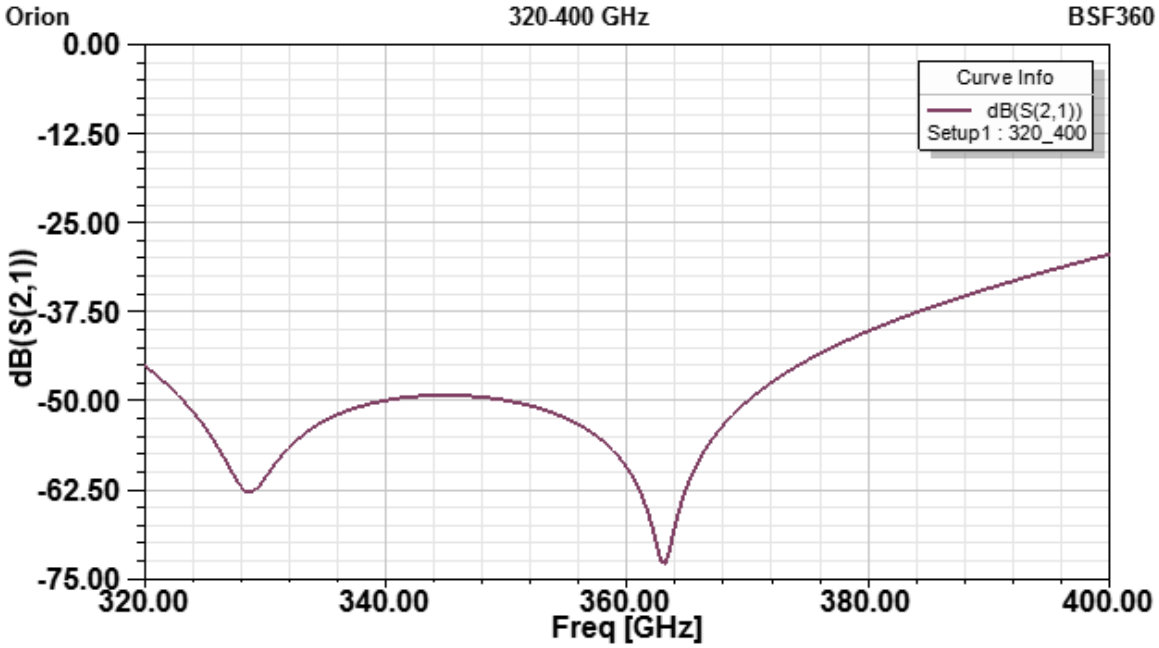

Figure 12. Transmission (S_{21}) and reflection (S_{11}) coefficients of a rejection filter at a frequency of 360 GHz obtained with HFSS.

5.2.3 Transition from a microstrip line to rectangular waveguide on diamond substrate

Figure 13 shows the design of transition from the microstrip line to a rectangular waveguide. Such a transition ensures transmission of microwave signal from the input (2) to the output (1). The main requirement for such a transition is minimization of losses at the output frequency.

The sizes of transition elements for frequencies 280 GHz and 360 GHz were obtained with HFSS. Shown in Figs. 14 and 15 are the transmission (S_{21}) and reflection (S_{11}) coefficients for the designs developed. One can see that the losses of that transition do not exceed 0.5 dB in both cases; this result is satisfactory.

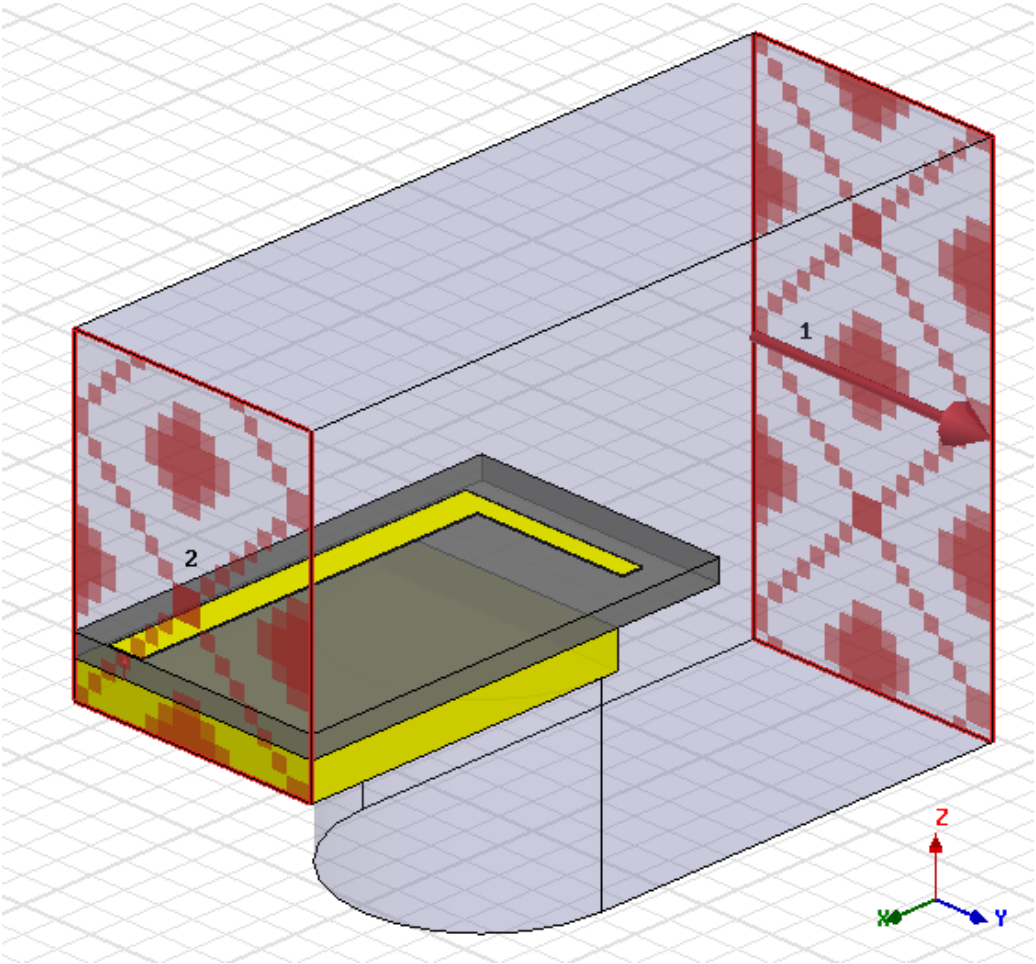

Figure 13. Design of a transition from a microstrip line to rectangular waveguide.

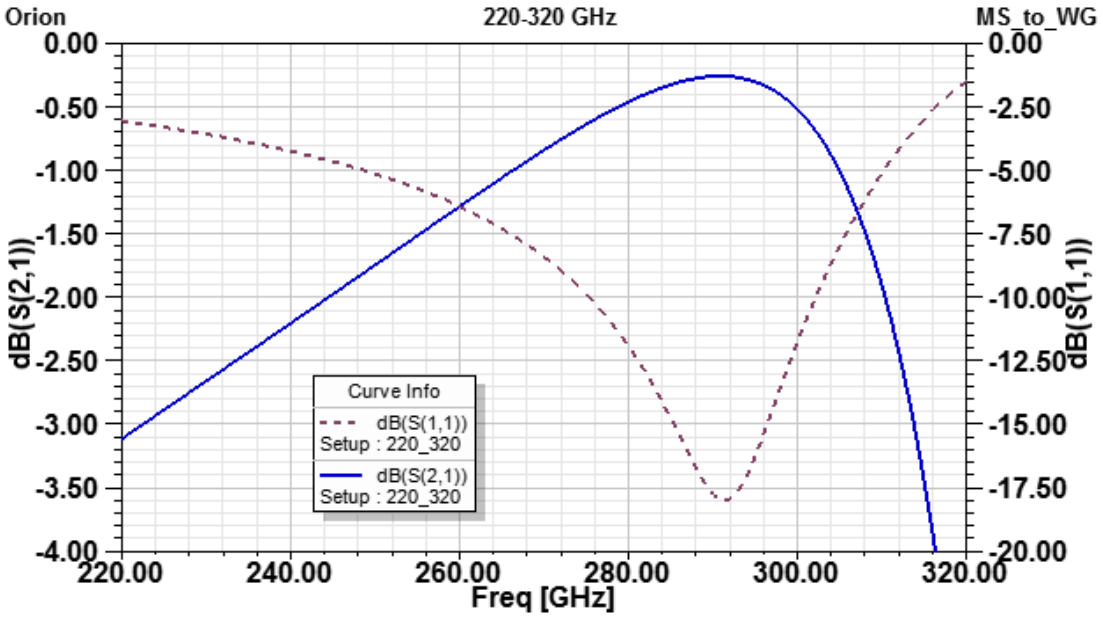

Figure 14. Transmission (S_{21}) and reflection (S_{11}) coefficients of a transition from a microstrip line to rectangular waveguide WR-03 obtained with HFSS.

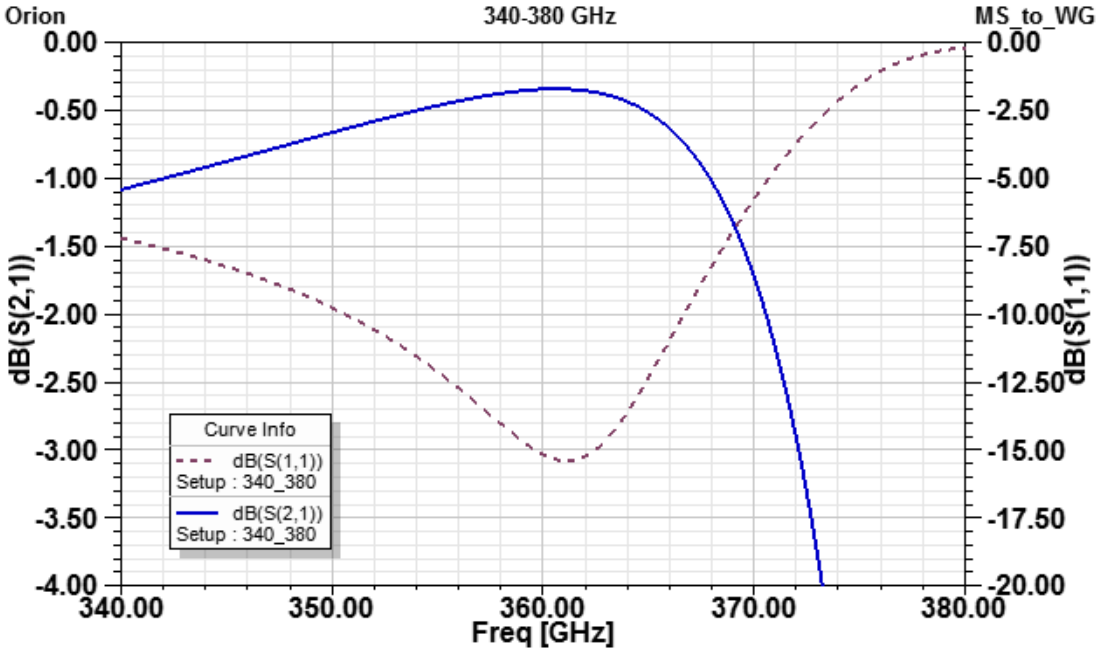

Figure 15. Transmission (S_{21}) and reflection (S_{11}) coefficients of a transition from a microstrip line to rectangular waveguide WR-2.8 obtained with HFSS.

5.2.4 Multiplier topology

Figure 16 shows the topologies of multipliers with an IMPATT diode and all the multiplier elements. The purposes and parameters of individual parts were described above. These topologies were used when designing photomasks intended for fabrication of IC prototypes.

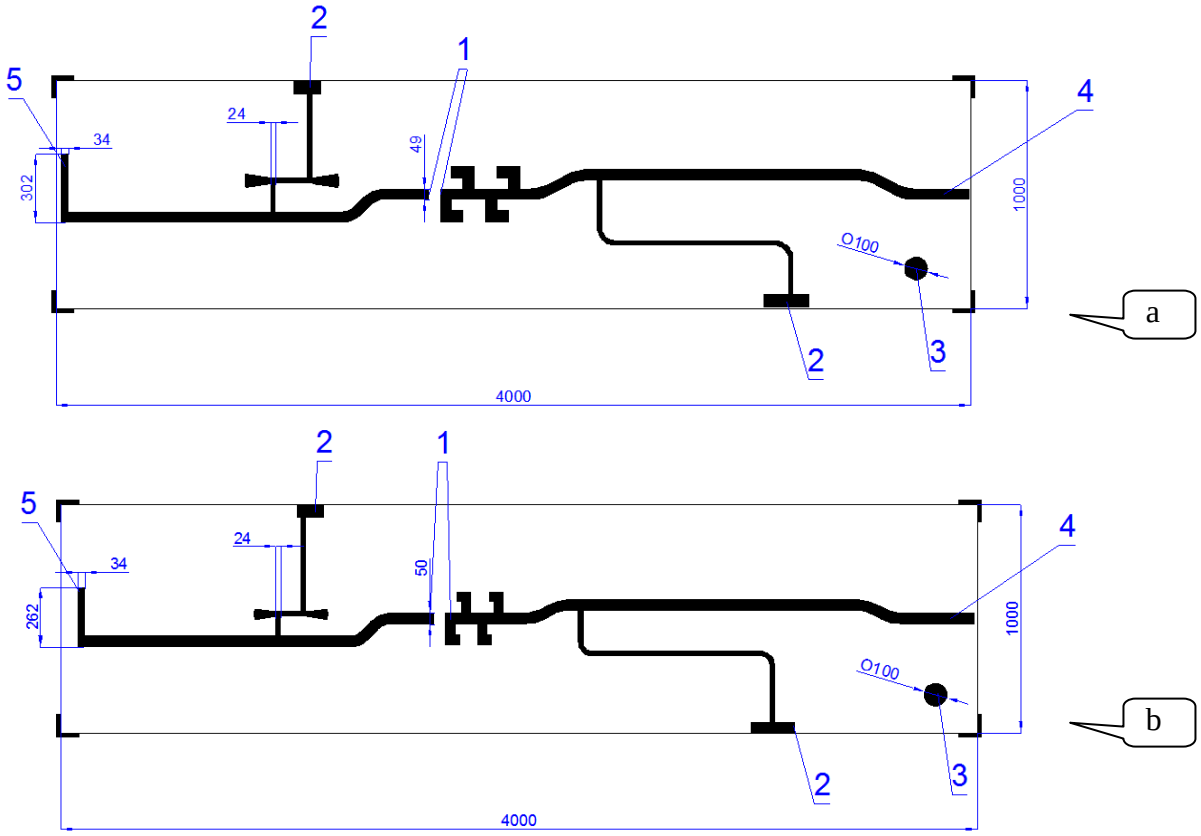

Figure 16. Topologies of multipliers with IMPATT diodes on diamond substrate 1 – silicon IMPATT diodes mounting sites, 2 – contact areas, 3 – test elements for adhesion control, 4 – microwave signal input, 5 – microwave signal output after frequency multiplication (a – 280 GHz, b – 360 GHz).

5.3 Technology development

We developed technological procedures for metallization systems intended for topology elements of microstrip ICs based on the Ti (0.05 μm)–Au (0.2 μm) and Ti (0.05 μm)–Pd (0.05 μm)–Au (0.1 μm)–Au (2–3 μm) metallizations. The manufacturing scheme for prototypes of ICs elements on diamond substrates has to involve the following stages:

- formation of IC topology,
- silicon IMPATT diode mounting into the IC topology elements,
- IC mounting into the package of functional module and provision of efficient heat removal from IMPATT diode to the package.

The topology elements and technology of IMPATT diode mounting are to ensure implementation of the key potential advantage of synthetic diamond, namely, minimal thermal resistance of IMPATT diode and long-term stability of this characteristic. Bearing the above-said in mind, mounting may be performed using diffusion welding

or gold–gold thermal compression. The optimal temperature for these processes lies within 350–380 °C.

The IC elements are to be made according to the manufacturing route (see Fig. 17) using initially the 15–45 μm synthetic diamond wafers on single-crystalline silicon substrates.

At first a ground plane (heat sink) of the microstrip transmission line is formed by sputtering of Cr–Cu layers (operations 1–3) and electrochemical growth of the Cu–Ni–Au system. Then the silicon substrate is etched off (operation 4) and the Ti–Pd–Au system is formed using vacuum sputtering (operations 5 and 6). After this, the microstrip transmission line topology is formed using electrochemical growth, photolithography and precise etching-out (operations 7–10). The wafer is cut into separate 1×1 mm^2 IC boards.

The results of elemental analysis of the initial samples of Ti–Au metallization system on synthetic diamond are presented in Fig. 18. One can see that, after etching for 10 min., we have a pure material made of carbon atoms (100%) (as is evidenced by the results of x-ray structural analysis of diamond), with high degree of structural uniformity. From analysis of morphological parameters of the diamond surface, it follows that both geometric and arithmetic mean roughness values for the surface under investigation are minimal. They practically do not change as the area considered is increased by nine times. The difference between the highest and lowest points of the scanned diamond surface is increased by 0.46 nm only as the area grows (see Figs. 19, 20, and 21). We did not found considerable contaminations by the elements analyzed. A smeared boundary of the Ti and C concentration depth profiles shows that some small mixture region may occur in the course of sputtering [7, 23, 24]. In our experiment, in the Ti layers (whose phase composition has been analyzed comprehensively in [6, 7, 25]) both carbon (up to 6%) and oxygen (up to 10%) are present over the whole film thickness.

The results of our investigation of the Ti–Pd–Au metallization system formed in a single process of vacuum sputtering are presented in Fig. 22. One can see that the carbon and oxygen contents in the sputtered Au and Pd layers are insignificant. Presence of carbon and oxygen was detected in the Ti layers as well as in the previous Au–Ti profiles. This is owing to high chemical activity of Ti layers.

We studied thermal stability of metallization systems used for topology elements based on Ti-Au and Ti-Pd-Au. Isothermal annealing was made at a temperature of 400 ºC for 5 min.; this corresponded to the conditions of microwelding and flux-free soldering. After such a thermal treatment, titanium and oxygen were detected at the surface of gold film in the Ti–Au metallization system. This was evidence that titanium diffuses through a thin Au layer to the surface and is oxidized. Such surfaces are not appropriate for microwelding and flux-free soldering. The elemental composition of the Ti–Pd–Au metallization system did not change at thermal treatment (400 ºC, 5 min.). The results of our investigations dictated the choice of the Ti–Pd–Au system for formation of topology of HIC elements on diamond surface.

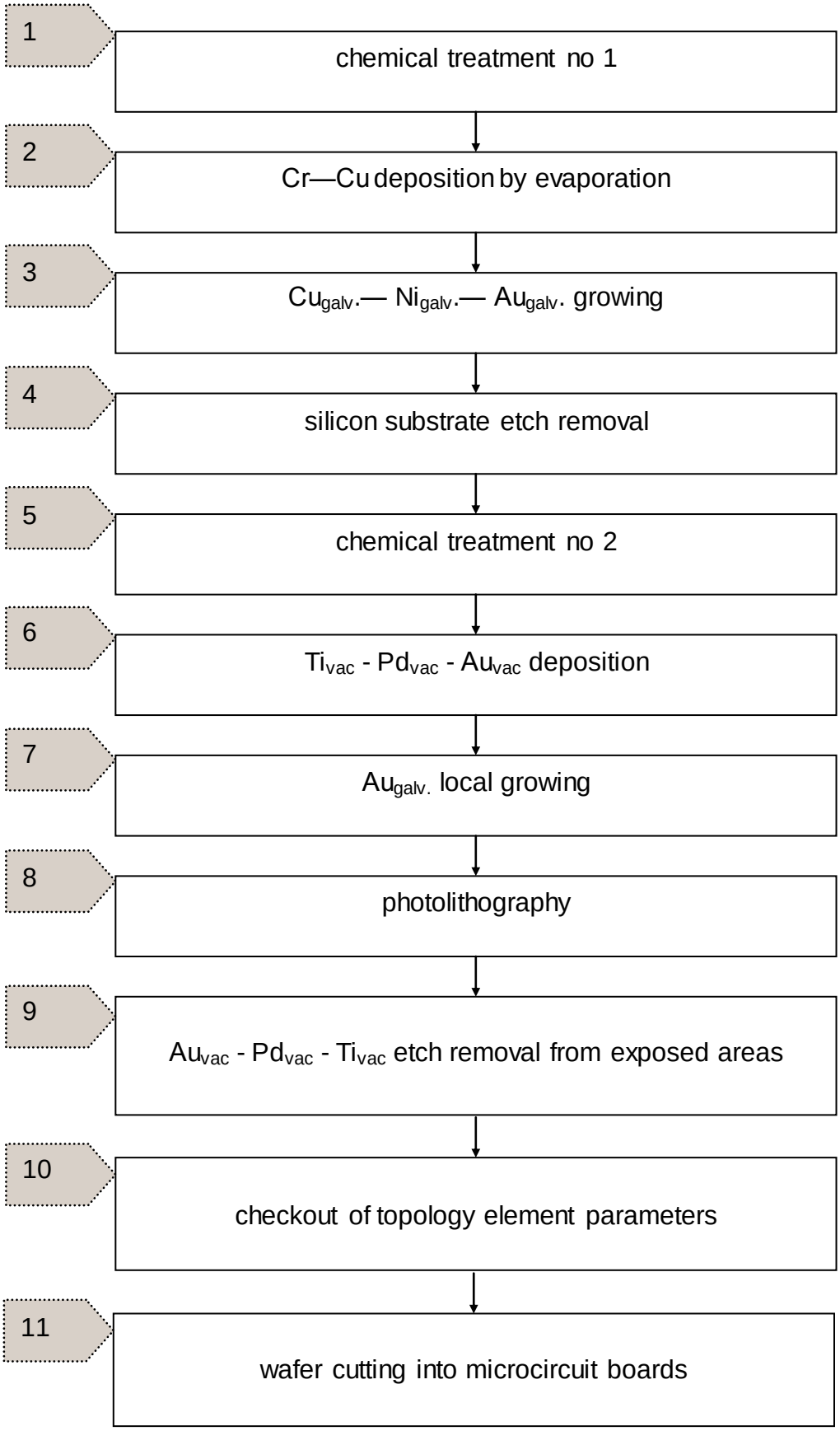

Figure 17. Manufacturing route diagram for IC on diamond substrate.

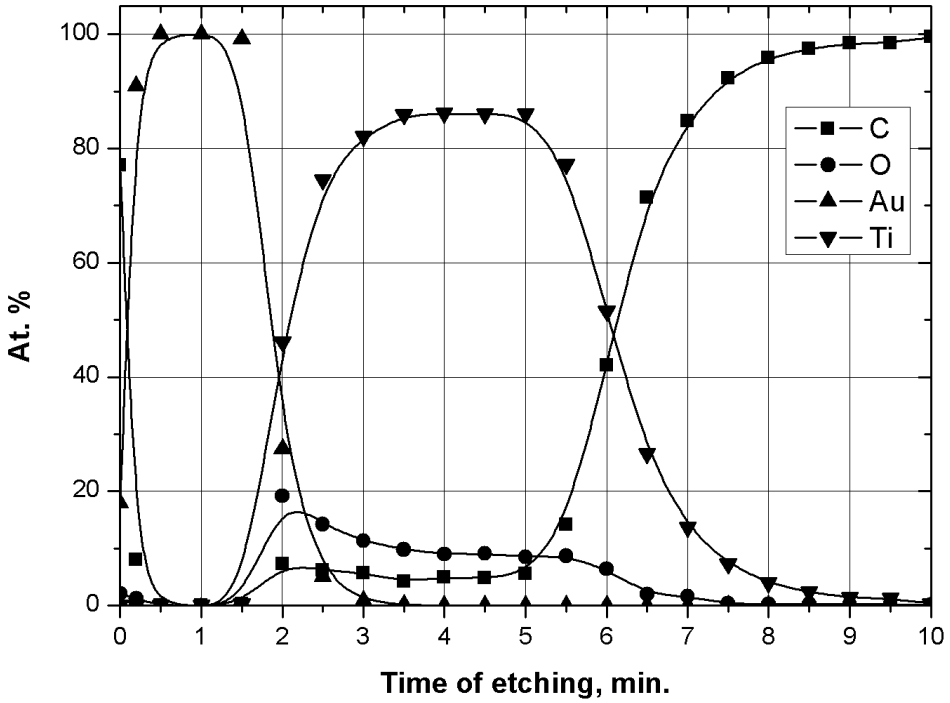

Figure 18. Auger concentration depth profiles in the Au–Ti metallization system on synthetic diamond after vacuum deposition at substrate temperature of 400 °C.

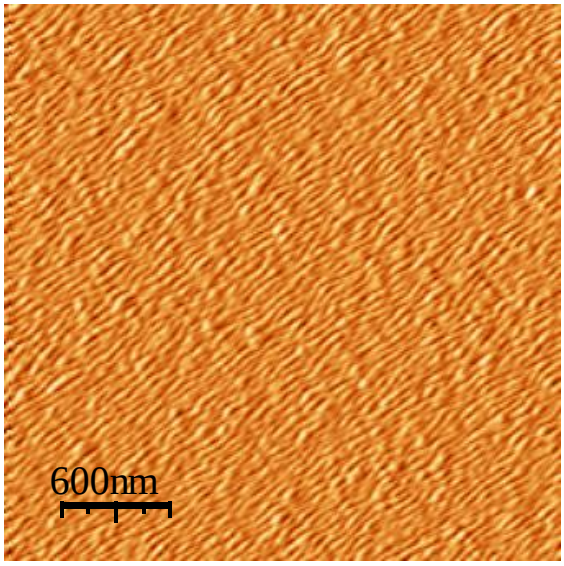

Figure 19. Diamond surface morphology after removal of Au–Ti metallization.

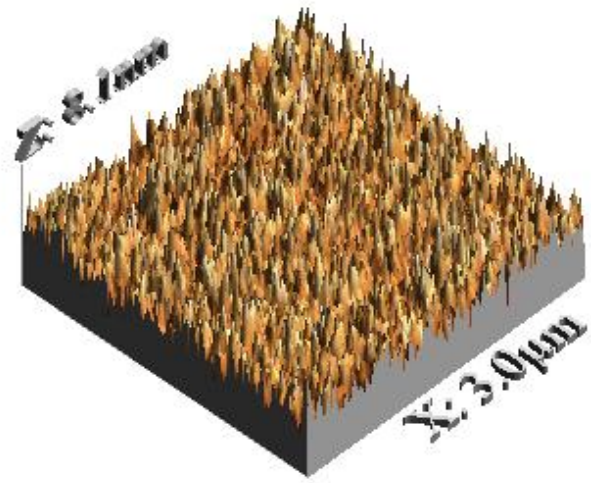

Figure 20. Diamond surface morphology after removal of Au–Ti metallization (axonometry).

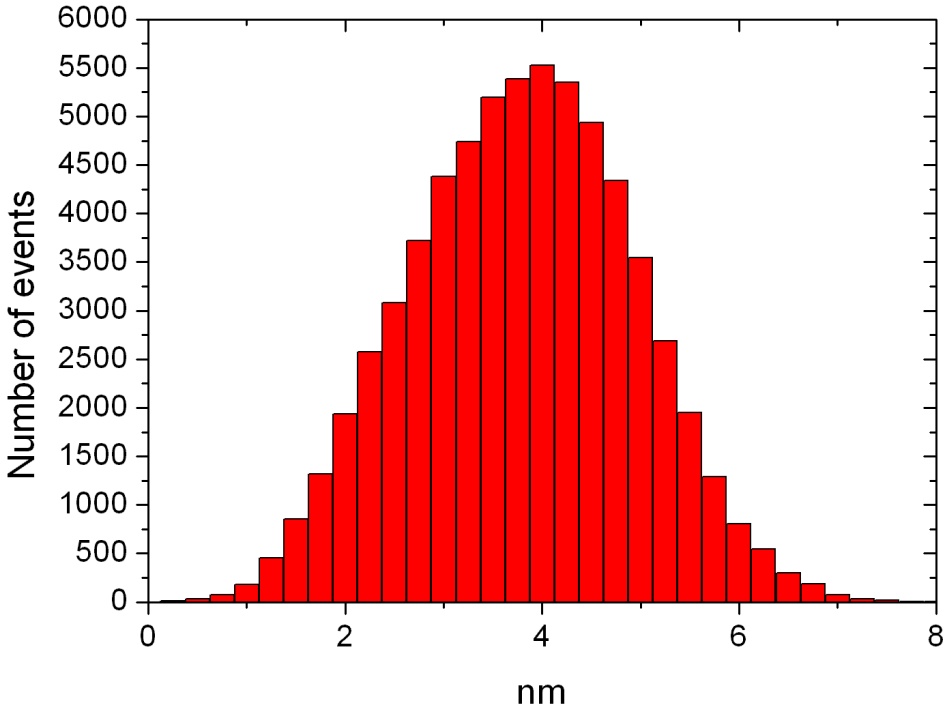

Figure 21. Histogram of diamond surface roughness heights after removal of Au–Ti metallization.

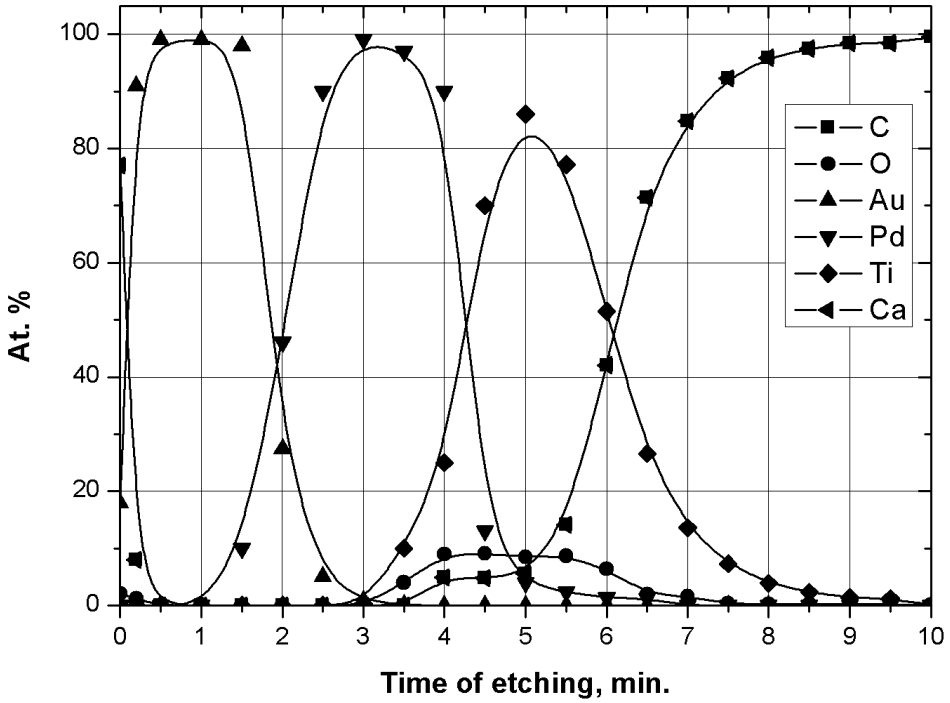

Figure 22. Auger concentration depth profiles in the Ti–Pd–Au metallization system on synthetic diamond after vacuum deposition at substrate temperature of 400 °C.

5.4 Manufacturing technology for ICs on diamond substrate

To form layout of the ICs that have been developed in the first quarter of the project, we made photomasks. They call for group manufacturing technology for ICs. A fragment of one of the photomasks is shown in Fig. 23.

We continued refinement of the technological processes using the photomask fabricated.

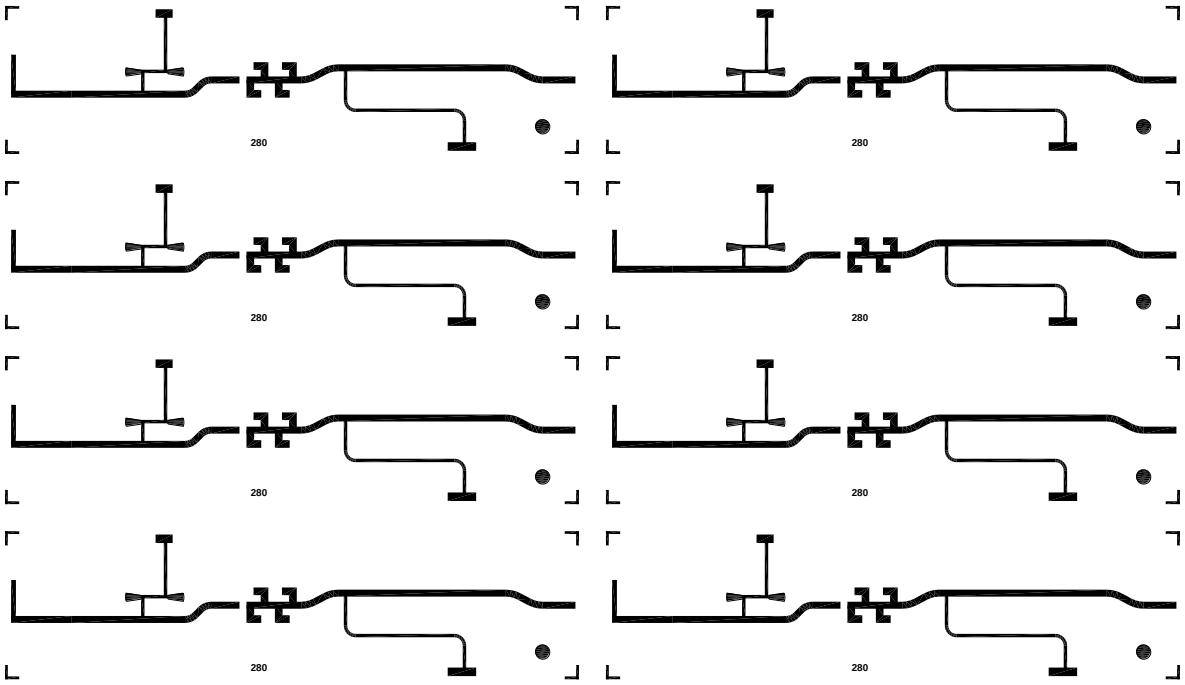

Figure 23. A fragment of photomask for microwave IC elements.

5.5 Manufacturing technology for IMPATT diode with beam leads

A manufacturing scheme based on the silicon thin membrane technology has been developed for diode fabrication. Such a manufacturing scheme should ensure minimal value of diode series resistance as well as possibility to regulate mesa diameter (and, therefore, capacitance) after diode assembly on IC using successive etching.

The manufacturing scheme for IMPATT diodes based on the membrane technologies is presented in Fig. 24. The proposed technology involved the following groups of operations [2, 3]:

- p^+- layer formation using precision diffusion of boron;
- etching of membrane (10±2) μm thick; etching on the n^+-layer side;
- double-sided diffusion of boron and phosphorus (formation of p^{++}- and n^{++}-regions);
- formation of contact areas to the p^+- and n^+-regions of Pd_2Si–Ti–Pd–Au-type using vacuum deposition (Pd_2Si is formed immediately in the course of the vacuum deposition of metal at a temperature of 330 °C);
- formation of beam leads 6÷9 μm thick using double-sided lithography and local deposition of gold layers;
- etching of the deposited Pd_2Si–Ti–Pd–Au metal layers;
- mesa etching.

After the last operation, the diodes are kept on the frame as is shown in Fig. 25.

We fabricated photomasks for realization of the manufacturing scheme. A set of photomasks ensures beam lead formation using the double-sided photolithography. The layout fragments for the upper and lower beam leads as well as fragment of coinciding photomasks layout are shown in Figs. 26 and 27, respectively.

The technological processes were refined in accordance with the manufacturing scheme developed.

The diffusion p^+-n junction was formed using boron diffusion from vapor phase at a temperature of 1150 ºC. The diffusion depth was about 0.5 μm, with boron near-surface concentration of 10^{20} cm^{-3}. Such surface concentration value ensured formation of good ohmic contact to the p^+-layer. The membrane was made using chemical-mechanical etching of the n^+-substrate; the final thickness of the n^+-layer was 8-9 μm. The total thickness of the membrane with all layers was 8-10 μm. To provide mechanical strength of the membrane at technological operations, a ring (width of 10 mm) was left along the peripheral region of the epitaxial structure at etching. The substrate resistance was 00015–0.0020 Ω·m; this corresponds to the dopant concentration of $(4–7)\times10^{19}$ cm^{-3}. It is difficult to obtain low-resistance ohmic contact at such concentration in the n^+-substrate [3]. Therefore, additional doping of the n^+-substrate up to surface concentration of about 10^{20} cm^{-3} was made (n^{++}-layer formation). The additional doping was made out of a solid source that was obtained from solution of tetraethoxysilane, ethanol and orthophosphoric acid H_3PO_4 [4]. The solution was applied on the n^+-layer with a centrifuge. After this thermal destruction of the deposited layer was performed at a temperature of 700-800 ºC. As a result, a thin (0.13-0.15 μm) layer of phosphorus-doped glass was obtained on the surface of the n^+-layer. The depth of additional doping with phosphorus was about 0.15 μm. The near-surface concentration in the layer obtained was such as to ensure transient resistance of the metal–semiconductor contact of about 10^{-6} Ω·cm [3].

The multilayer Pd–Ti–Au system served as ohmic contacts to the heavily doped layers. Palladium and silicon form palladium silicide Pd_2Si at a temperature of 400 ºC, thus ensuring high reliability of the contacts. All the above metallization layers were about 0.1 μm thick. They were formed using vacuum deposition; the substrate (membrane) temperature was 300 ºC.

The windows for beam leads were formed on both sides of the metallized membrane using the double-sided lithography with photoresist deposition. A gold layer 6-8 μm thick was electrodeposited in the beam lead windows.

The mesas (30-50 μm in diameter) were etched in the semiconductor membrane with beam leads. All the diodes were connected (on the upper lead side) with thin gold jumpers that are separated in the course of diode cutting.

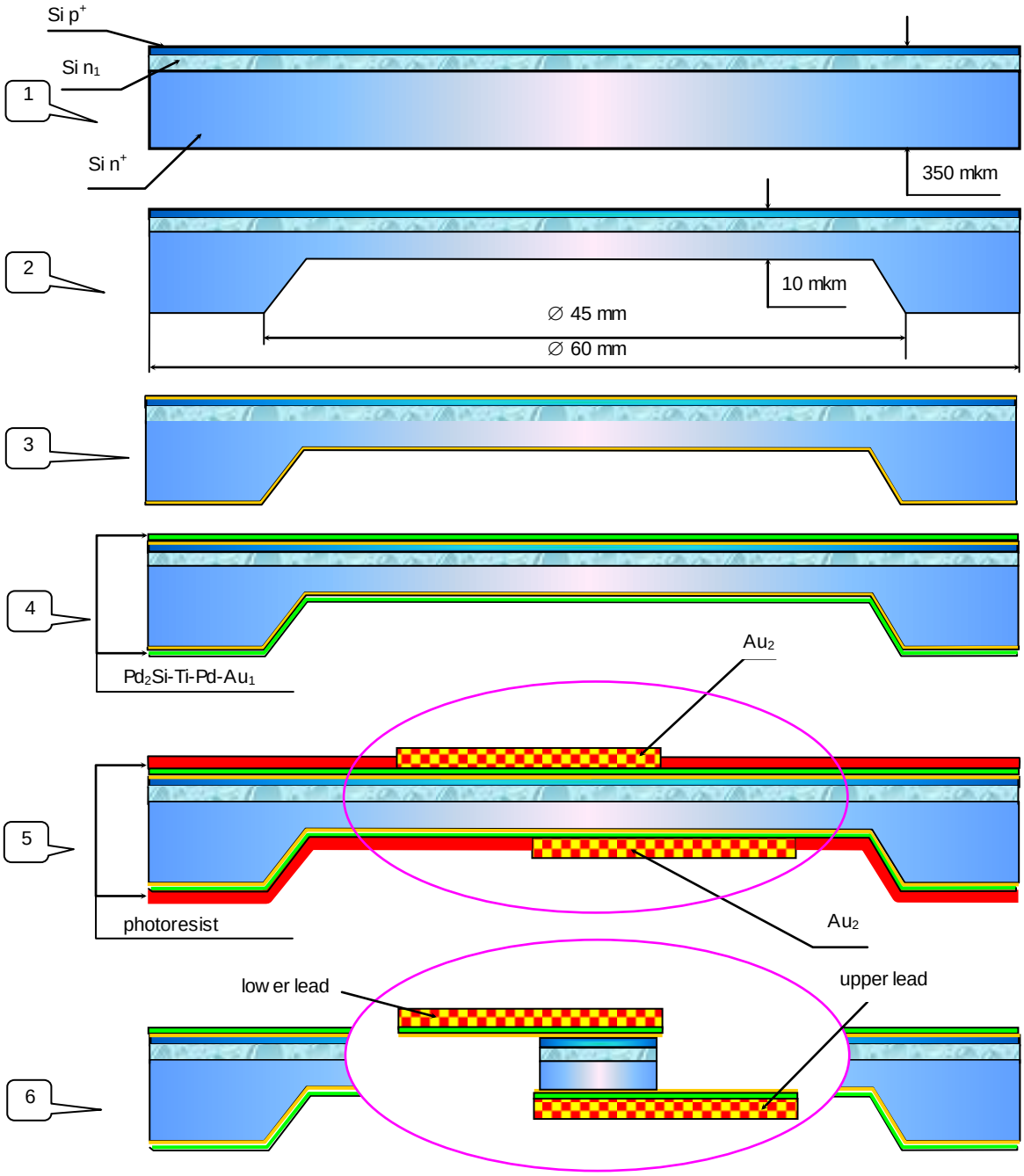

Figure 24. Manufacturing scheme for silicon IMPATT diodes with beam leads. **1** – p^+-layer formation using precise diffusion of boron; **2**– etching of membrane (10 ±2) μm thick, etching on the n^+-layer side; **3** – double-sided diffusion of boron and phosphorus (formation of p^{++}- and n^{++}-regions); **4** – deposition of contact systems to the p^+- and n^+-regions of Pd_2Si–Ti–Pd–Au-type; **5** – formation of beam leads 6÷9 μm thick using local deposition of gold layers; **6** – etching of sputtered metal layers and mesa etching.

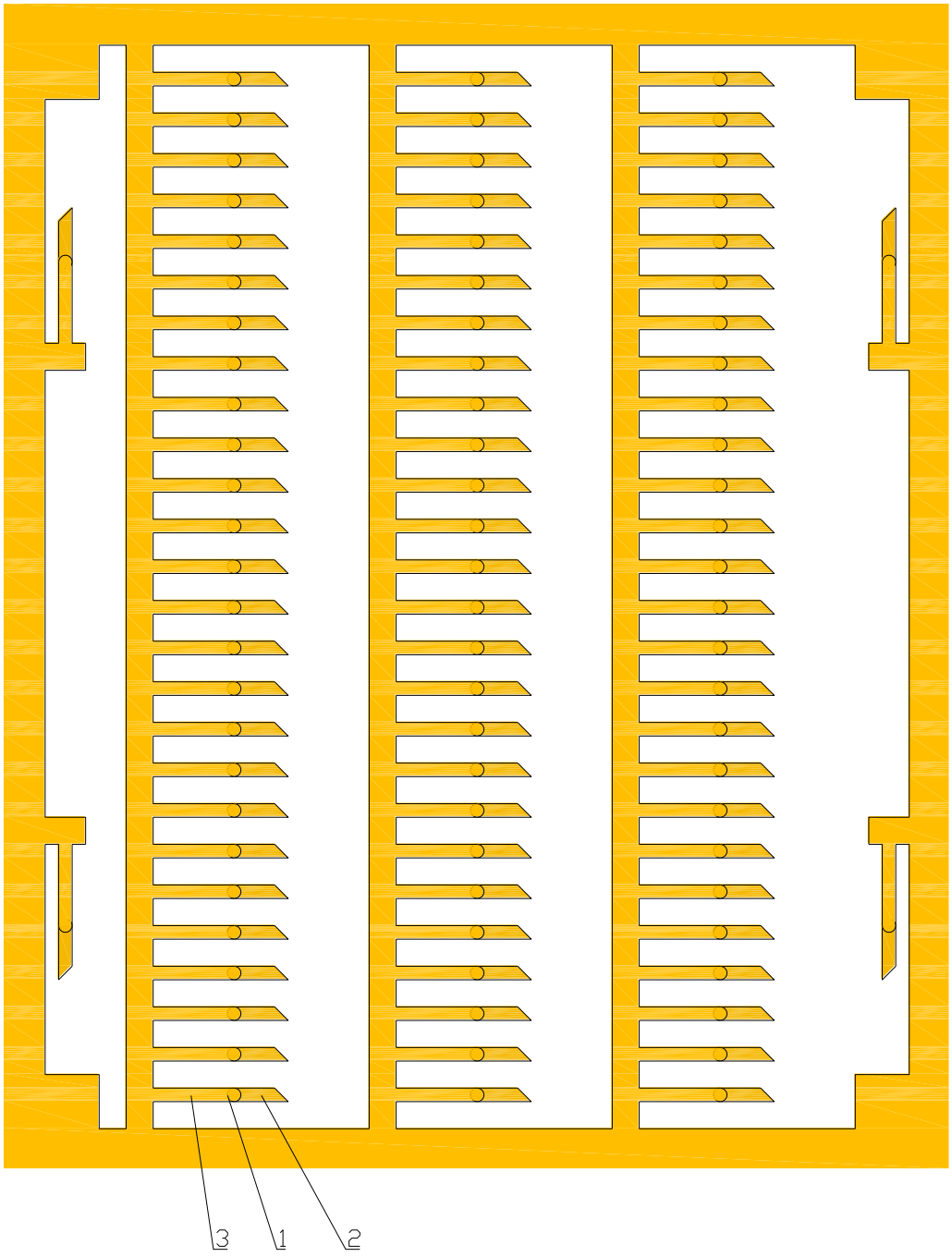

Figure 25. A magnified fragment of single section supporting IMPATT diodes after mesa etching.
1 – mesa, **2** – lower contact, **3** – upper contact.

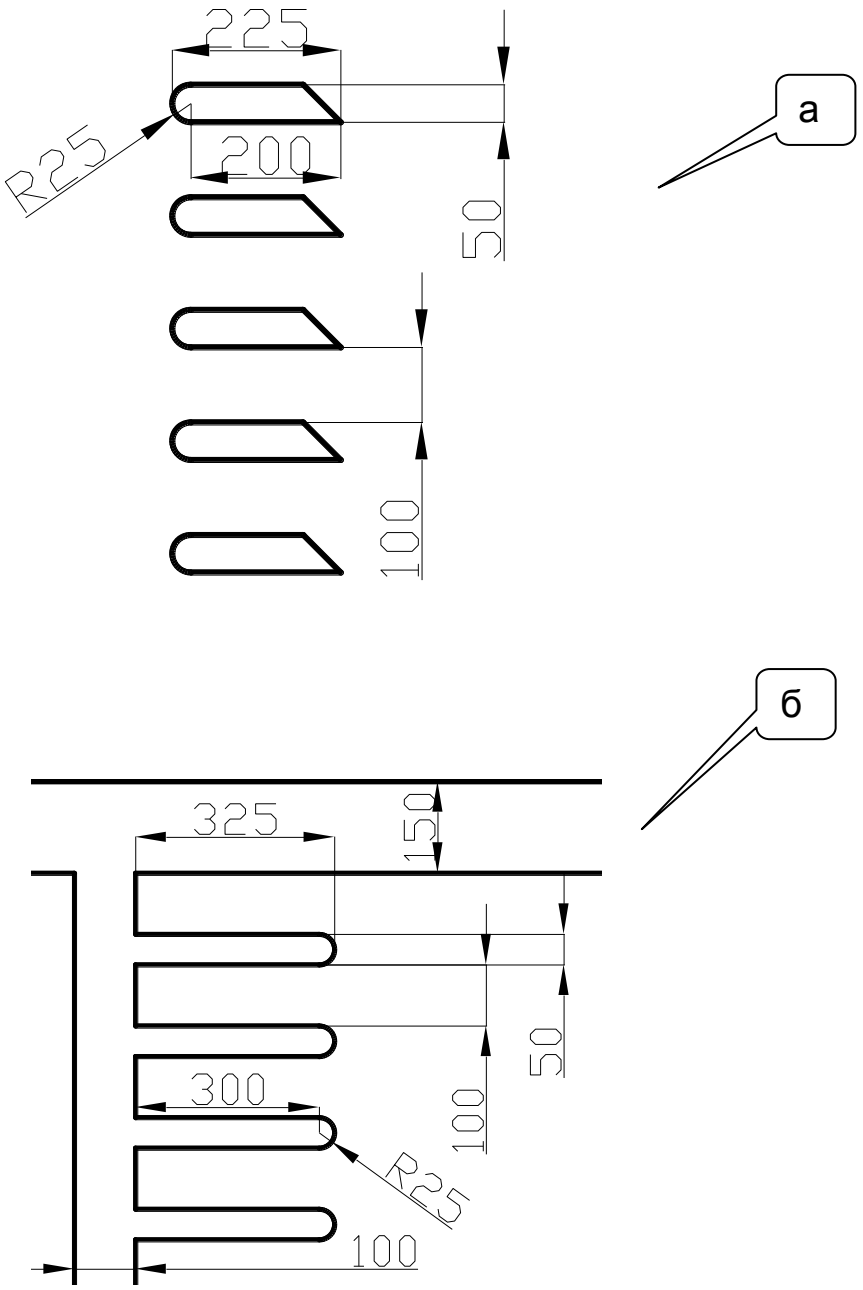

Figure 26. Layout fragments for the lower (a) and upper (b) diode beam lead.
(The sizes are given in microns.)

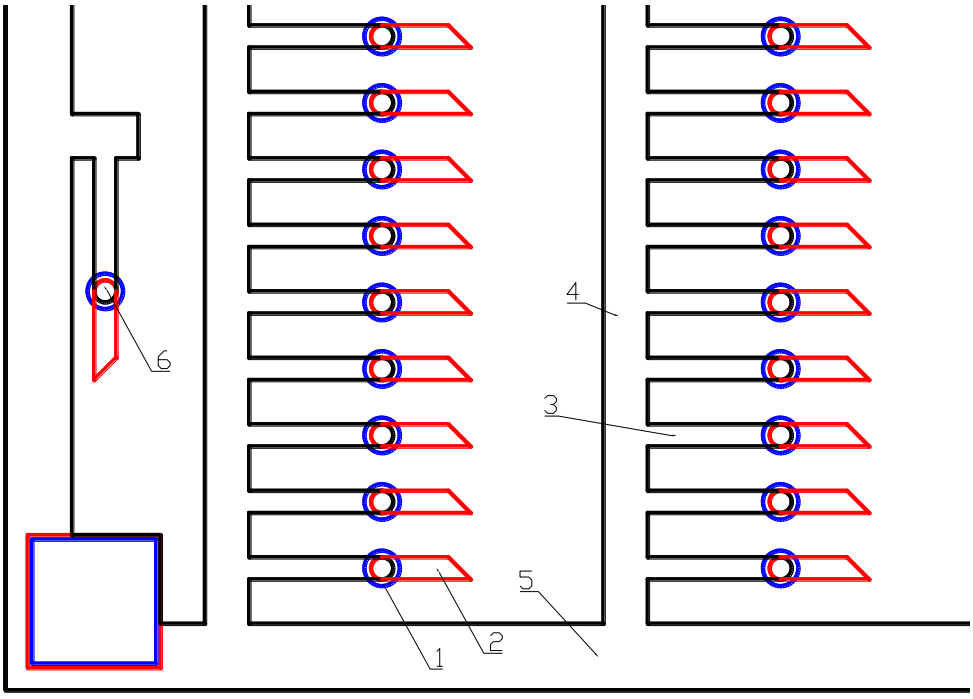

Figure 27. A fragment of photomasks coincidence plan for fabrication of IMPATT diodes.
1 – mesa, **2** – lower beam lead, **3** – upper beam lead, **4** – supporting strips, **5** – section frame, **6** – test element.

5.6 Manufacturing of experimental ICs on diamond substrate

We made multiplier microstrip boards on diamond substrates and studied their characteristics. A photograph of the microstrip board is presented in Fig. 28.

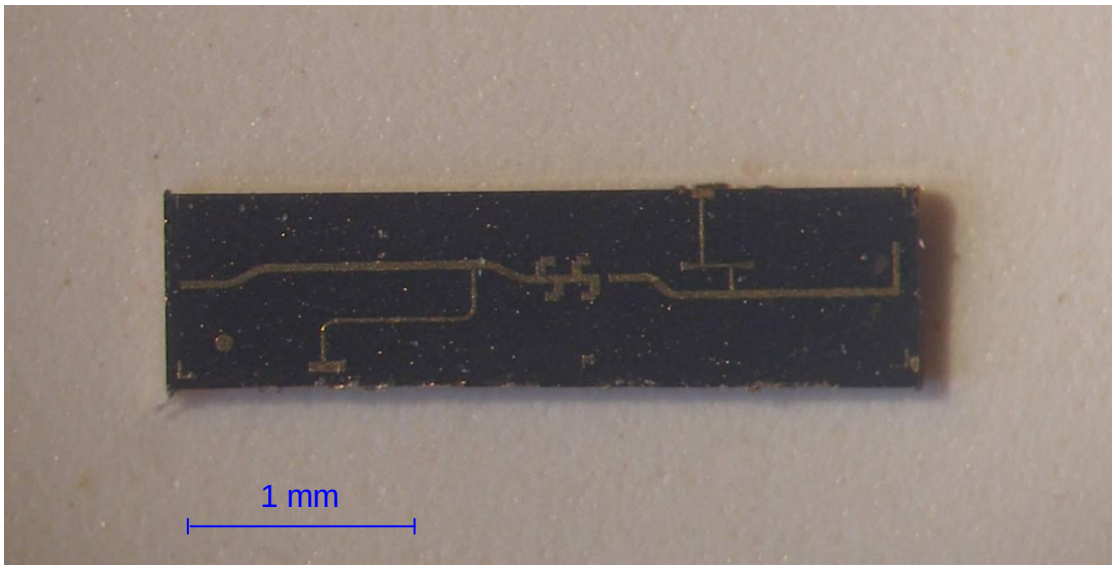

Figure 28. Photograph of a microstrip board on diamond substrate.

5.7 Electrical characteristics and parameters of metal-diamond-metal structure

Figures 29 and 30 show the *I-V* curves taken at 20°C and in the 20-400°C temperature range, respectively. One can see that the currents through the metal-diamond-metal structures grow with temperature.

As temperature is increased from +25ºC up to +400ºC, the order of current through the structure grows from 10^{-9} A up to 10^{-2} A. To illustrate, at diamond temperature of 400ºC and capacitor voltage of 260 V, the currents are as high as 2÷3 mA. The current growth with temperature is due to decrease of resistance of the metal-diamond-metal structure. The resistivity ρ of synthetic diamond was determined from the expression

$$\rho = \frac{\Delta U \cdot S}{\Delta I \cdot d}.$$

Here S is the area of the metal-diamond- metal structure, d the diamond layer thickness. The temperature dependence of the *I-V* curve is nonlinear, so ΔU was determined for two sections of the *I-V* curve, namely, ΔU_1 =50 V – 25 V = 25 V and ΔU_2 = 300 V – 100 V = 200 V. Shown in Fig. 31 are the temperature dependences of diamond resistivity. One can see from Fig. 31 that, as temperature grows, the resistivity of the metal-diamond-metal structure decreases from 10^{12} Ω·cm down to 5×10^{6} Ω·cm. Such temperature dependence is characteristic of the semiconductor structure.

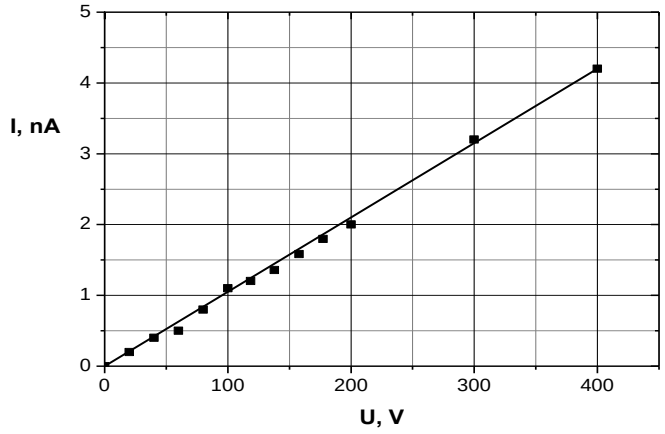

Figure 29. *I-V* curve of metal-diamond-metal structure at 20°C.

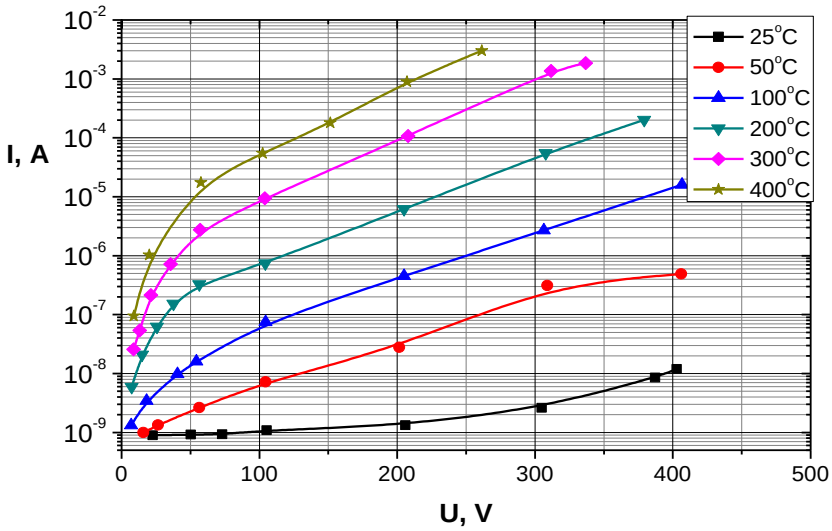

Figure 30. *I-V* curves of metal-diamond-metal structure taken in the 25-400°C temperature range.

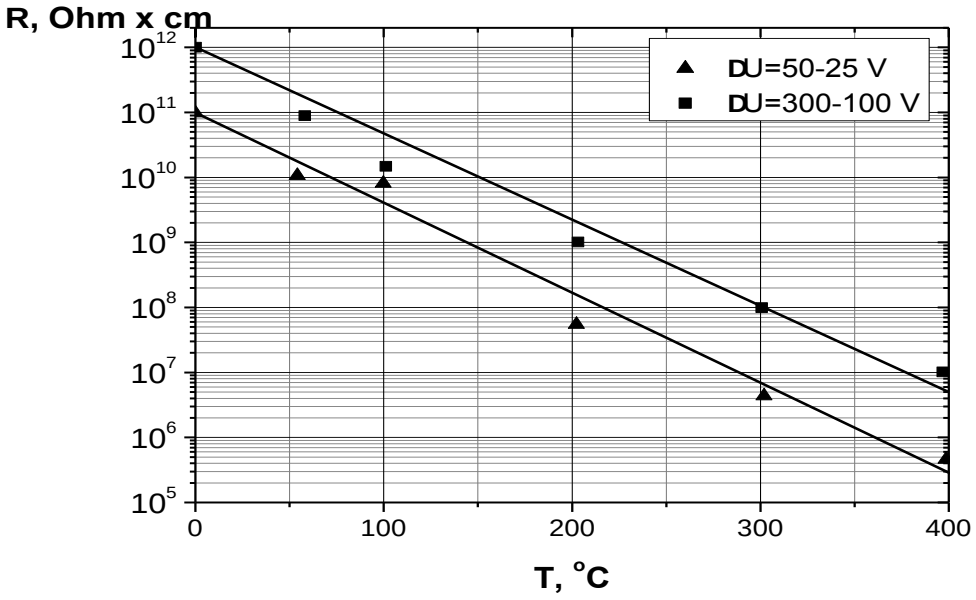

Figure 31. Temperature dependence of metal-diamond-metal structure resistivity at electric field strength up to 5×10^4 V/cm.

The effective capacitance of the metal-diamond-metal structure was measured with a E7-12 device at a frequency of 1 MHz in the 25÷400ºC temperature range. It was found that the capacitance did not depend on voltage in the 0÷40 V range. Shown in Fig. 32 is the temperature dependence of capacitance *C* of the metal-diamond-metal structure taken at capacitor voltage of 10 V.

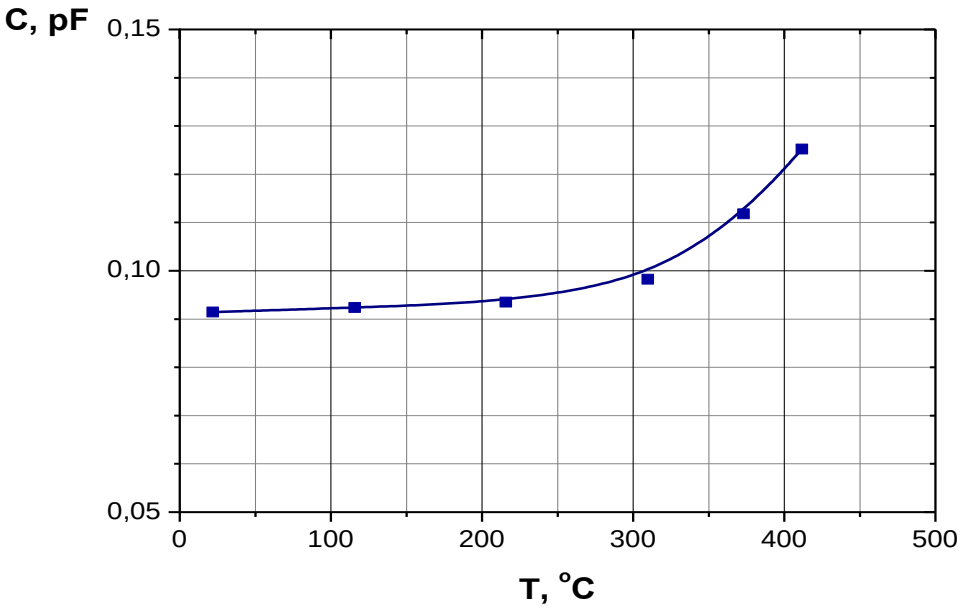

Figure 32. Temperature dependence of metal-diamond-metal structure capacitance at *U* = 10 V

One can see from Fig. 32 that the structure capacitance grows at temperatures over 300ºC. This is because of decrease of diamond resistivity.

Knowing the value of capacitance *C* for the metal-diamond-metal test structure, we estimated the thickness of diamond substrate, d_c from the expression $C = S\varepsilon/d$ (where *S* is the structure area, *d* thickness of dielectric substrate and ε permittivity) and compared it to the results of substrate thickness measurement with a microscope (d_M). The results of measurements performed for two wafers are presented in Table 1.

Table 1

Wafer #	*C*, pF	d_c, μm	d_M, μm
1	0.102	14.21	14÷15
2	0.088	16.47	14÷15

One can see that the results obtained with a microscope and from the capacitance value are in good agreement.

5.8 Strength of metal-diamond joint

Our investigations obtained for the Ti-Pd-$Au_{sputt.}$-Au_{galv} (3 μm) metallization system showed that the force per unit area that is required for break-off of the control contact pad from diamond substrate is no less than 130 kg/cm^2. Performance of microassembly operations with HIC module heating up to a temperature of 350ºC did not reduce adhesion strength.

5.9 Manufacturing technology for beam-lead IMPATT diodes

We made the laboratory models of silicon beam-lead IMPATT diodes. Shown in Fig. 33a is a silicon wafer in whose central region the beam-lead IMPATT diodes are formed. Figure 33b shoes an enlarged fragment of that region. For further process operations and studies, the diodes are cut off under the microscope.

5.10 Characteristics and parameters of IMPATT diodes mounted in microwave package

We studied the *I-V* and *C-V* curves and differential resistance R_d (at forward current) of silicon beam-lead IMPATT diodes to be mounted in the frequency multiplier IC chips formed on diamond substrates.

The typical diode characteristics (taken before and after etching) are presented in Figs. 34-36. The dynamics of variation of IMPATT diode capacitance and resistance is shown in Figs. 37-38.

One can see from the results presented in Figs. 37 and 38 that it is possible to reduce smoothly the IMPATT diode capacitance by a factor of 2.5-2.6 using additional etching of silicon mesa. One can follow capacitance variation from that of differential resistance. In this way, smooth variation of capacitance of IMPATT diodes mounted in IC chip on diamond substrate is ensured.

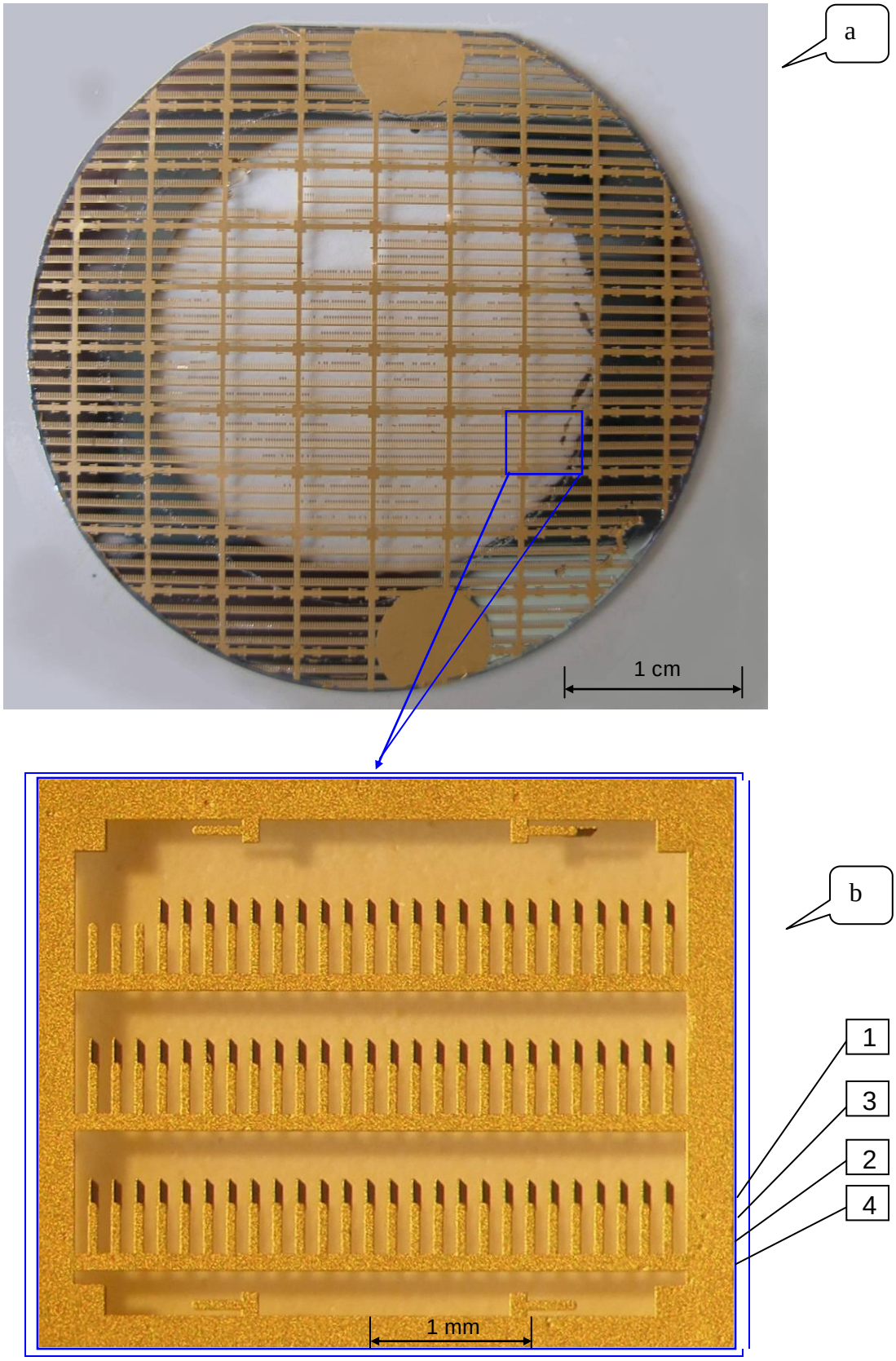

Figure 33. Photograph of a wafer with diodes (a) and enlarged fragment of the region with beam-lead IMPATT diodes (b):
1 – lower contact, 2 – upper contact, 3 – silicon mesa of IMPATT diode, 4 – site of diode cut.

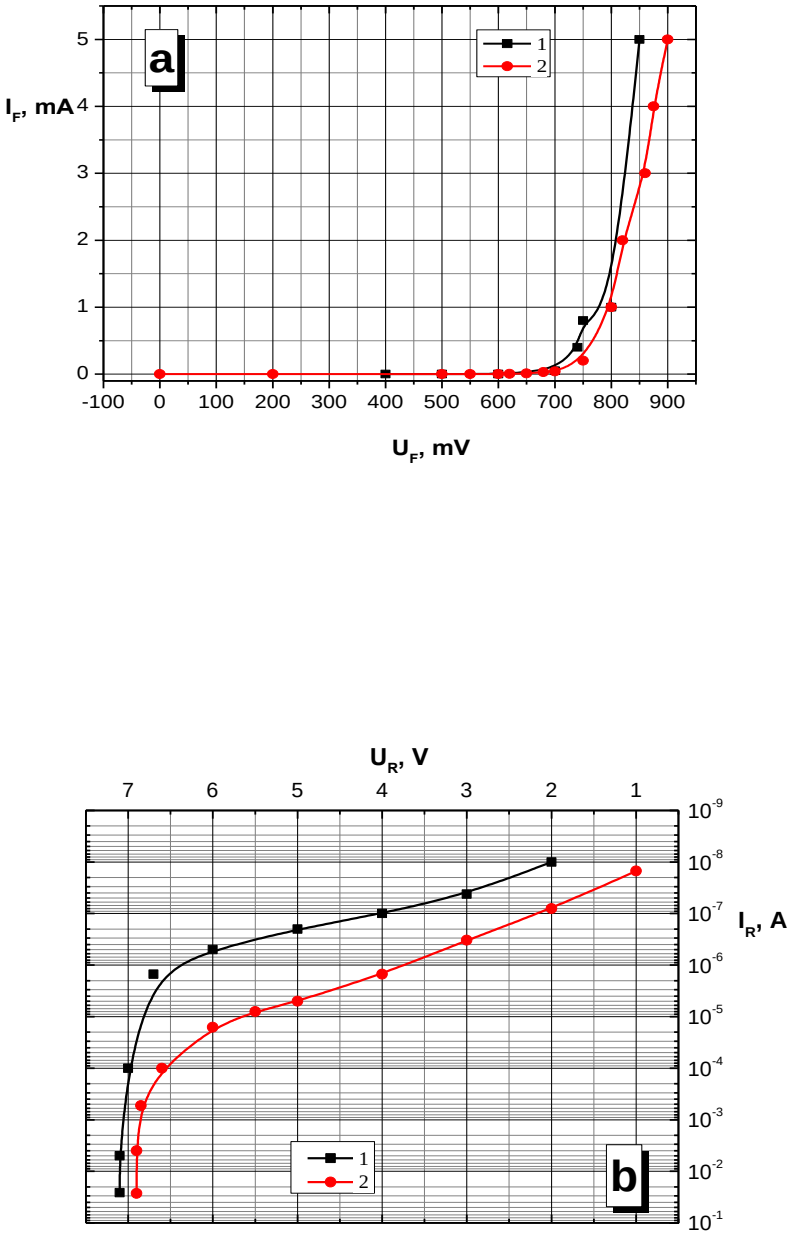

Figure 34. *I-V* curves of beam-lead IMPATT diode model before etching. a – forward branch, b – reverse branch: 1 – initial sample, 2 – after additional etching of silicon mesa for 7 sec.

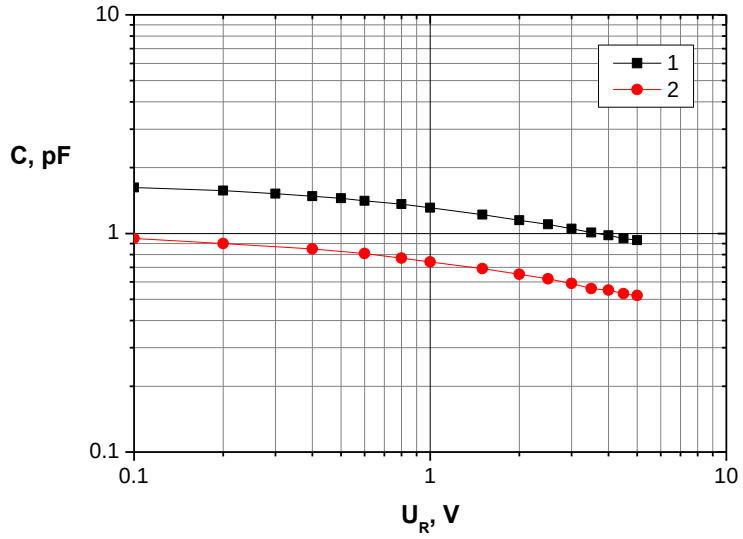

Figure 35. Capacitance (C) of beam-lead IMPATT diodes as function of reverse voltage (U_R).
1 – before etching, 2 – after silicon mesa etching for 7 sec.

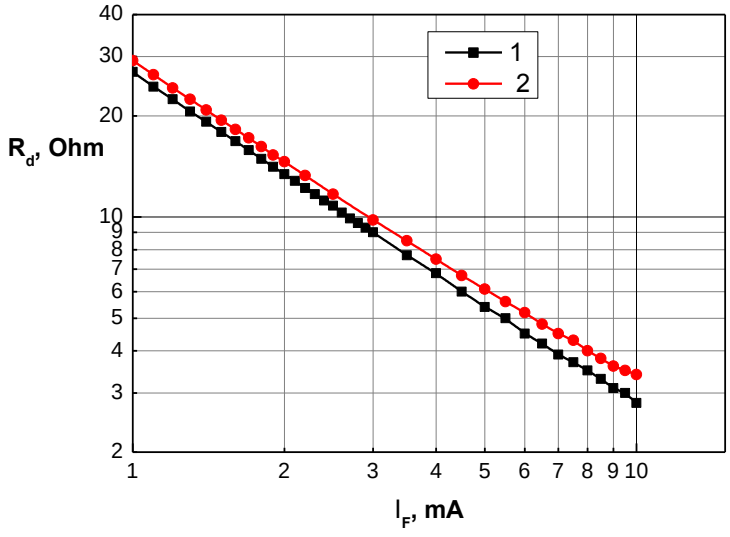

Figure 36. Differential resistance (R_d) of beam-lead IMPATT diode model as function of forward current (I_F).
1 – before etching, 2 – after silicon mesa etching for 7 sec.

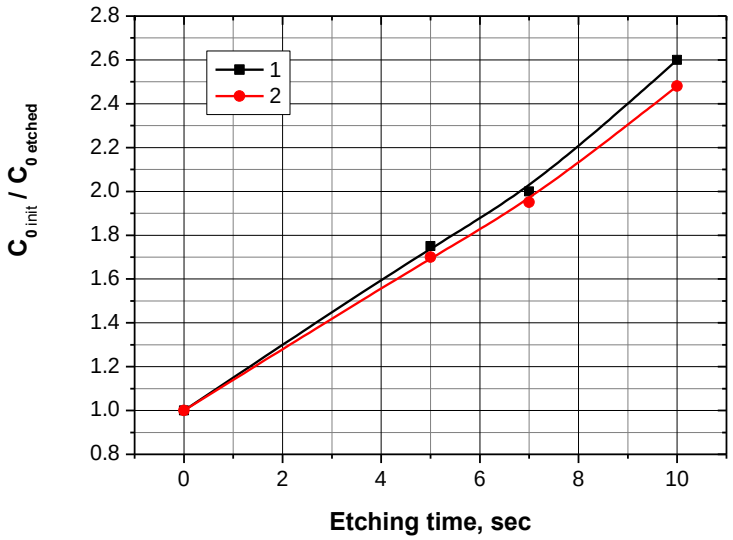

Figure 37. Capacitance variation (C_0 init/C_0 etch) of two beam-lead IMPATT diodes (1, 2) as function of etching time.

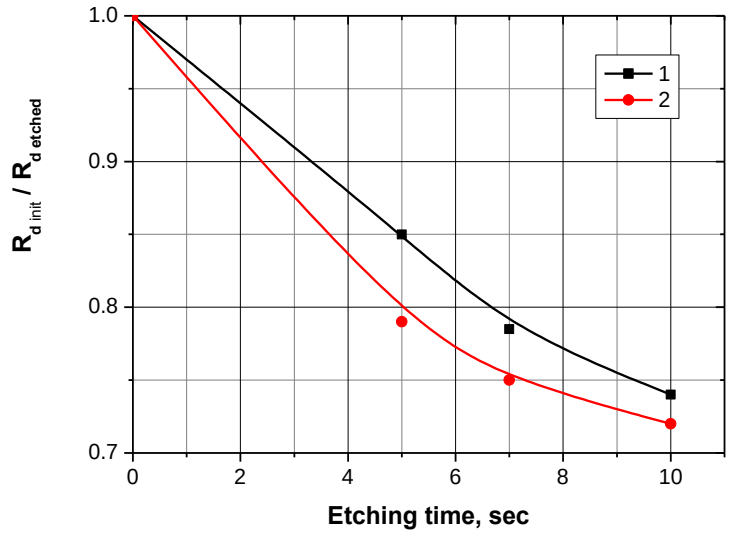

Figure 38. Differential resistance variation (R_d init/R_d etch) of two beam-lead IMPATT diodes (1, 2) as function of etching time.

5.11 Characteristics and parameters of IMPATT diodes mounted in IC

The *I-V* curves for IMPATT diodes mounted in HIC chips on diamond substrates (taken after additional mesa etching during 7 sec) are shown in Fig.39.

From the results presented it follows that the parameters of *I-V* curves of IMPATT diodes after mounting in IC chip and additional mesa etching are the same as those of the diode models mounted in microwave package.

The typical dependences of differential resistance R_d of IMPATT diodes mounted in IC chips on etching time are presented in Fig. 40.

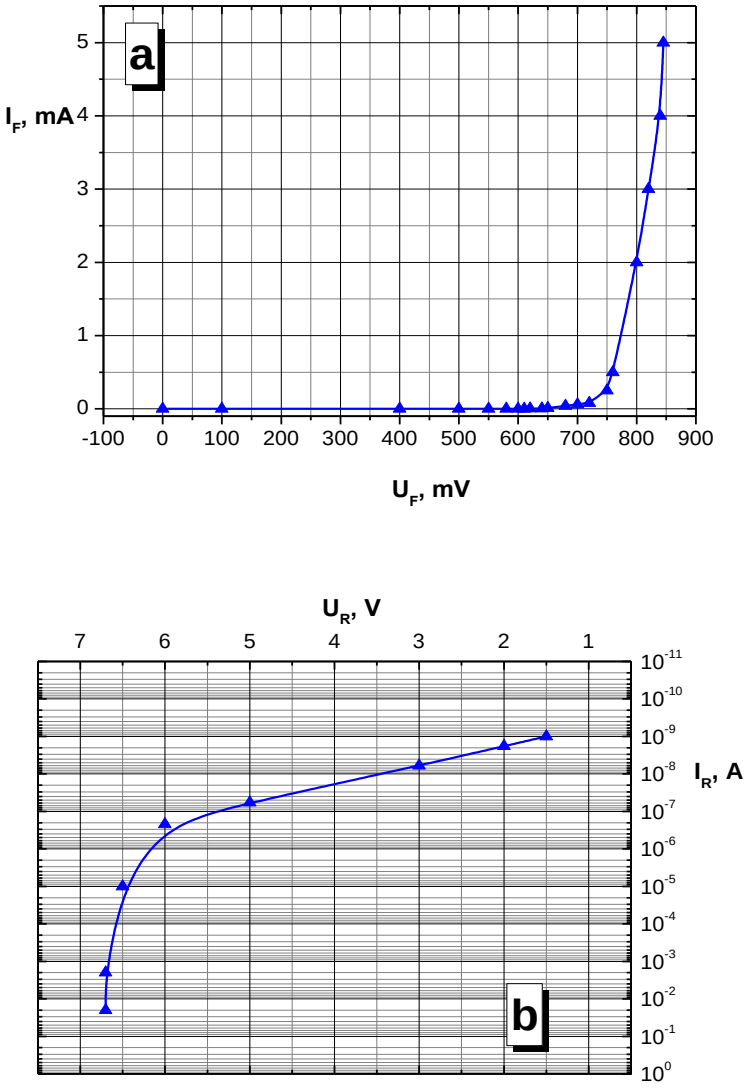

Figure 39. *I-V* curves of beam-lead IMPATT diodes mounted in HIC on diamond substrate after etching for 7 seconds.
a – forward branch, b – reverse branch.

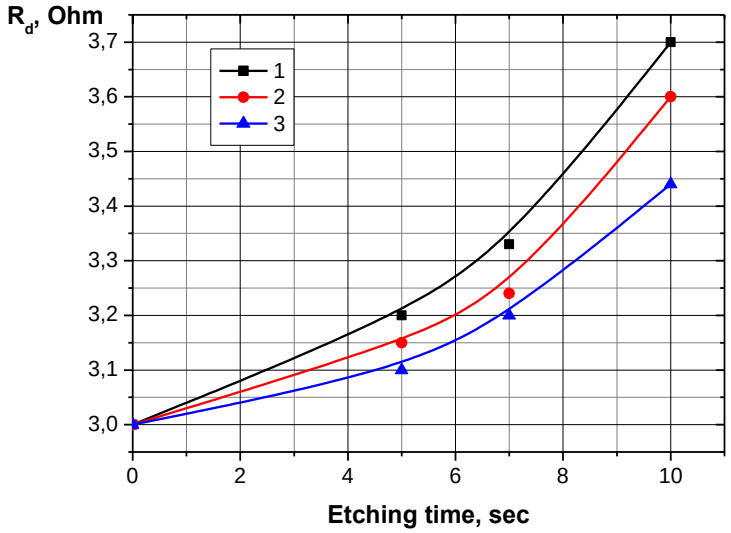

Figure 40. Differential resistance (R_d) of three beam-lead IMPATT diodes mounted in HIC on diamond substrate as function of etching time at forward current of 10 mA.

From the above results it follows that, after additional mesa etching, the parameters of *I-V* and *C-V* curves of beam-lead IMPATT diodes mounted in the chip of multiplier IC on diamond substrate ensure the possibility to use such diodes as active elements of frequency multipliers. By additional etching, one can vary over wide range the IMPATT diode differential resistance and, consequently, its capacitance. In this case, the main IMPATT diode characteristics (the breakdown voltage and parameter stability at avalanche breakdown) remain the same.

6 Conclusions

A frequency multiplier with IMPATT diode having high multiplication ratio served as a device demonstrating the advantages of diamond application as substrate. We chose output frequencies of 280 GHz and 360 GHz to perform analysis and calculations as well as for experimental studies.

Choosing of diamond substrate thickness makes a complex problem. On the one hand, one should decrease the dielectric thickness as frequency grows to reduce the transmission line width. On the other hand, in that case the transmission line losses increase. Thus, the above problem is to be considered separately for each specific application. In this project, we chose diamond thickness of 30 μm for multiplier realization.

The successful development and simulation of the elements of frequency multiplier with high multiplication ratio that have satisfactory parameters indicate possibility of realization of ICs on diamond substrates.

In the course of our studies it was found that the Ti–Pd–Au metallization system (thickness of 2–3 μm) can be applied when forming the topology of IC elements on

synthetic diamond layers, while the Cr–Cu–Ni–Au metallization system with thick (up to 50 μm) copper layer can serve as screen heat sink and HIC elements carrier.

We did not found considerable interaction processes in the Ti–Pd–Au metallization layers at temperatures up to 400 ºC. This indicates its rather high thermal stability and possibility of application in technological processes of microwelding and flux-free soldering at temperatures up to 400 ºC.

The technical documentation on fabrication of photomasks for IC topology formation in frequency multipliers with silicon IMPATT diodes with operating frequencies of 280 GHz and 360 GHz was developed.

A construction of IMPATT diode was developed. It is a n^{++}-n^{+}-n-p^{+}-p^{++}-mesa with gold beam leads. The initial mesa diameter is 40 μm, while the beam lead thickness is 6 μm. We plan to reduce the mesa diameter to 12÷15 μm using successive etching after diode assembly on the IC chip.

A manufacturing scheme for IMPATT diode based on the silicon thin membrane technology was developed. The photomasks were designed and fabricated to realize the manufacturing scheme. A set of photomasks ensures formation of beam leads and mesas using the double-sided photolithography. The technological processes were refined in accordance with the manufacturing scheme.

The photomasks to form IC layout were made. They call for group manufacturing technology for ICs with a common integrated heat sink that ensures also mechanical strength of a wafer with ICs.

The investigations of test elements of transmission lines of microwave ICs showed that the resistivity of synthetic diamond substrate is no less than 1×10^{12} Ω·cm (10^{7} Ω·cm) at a temperature of +25°C (400ºC) at electric field no more than 5×10^{4} V/cm.

Since resistivity of the metal-diamond-metal structure decreases considerably and its effective capacitance increases as temperature grows in the 25÷400ºC range, the highest operating temperature of the transmission line elements on synthetic diamond is determined to be 300°C.

Our studies for the Ti-Pd-Au_{sputt}-Au_{galv} (3 μm) metallization system showed that the force per unit area that is required for break-off of the control contact pad from diamond substrate is no less than 130 kg/cm^2. Performance of microassembly operations with HIC module heating up to a temperature of 350ºC does not reduce adhesion strength.

The silicon beam-lead IMPATT diode parameters (differential resistance and capacitance) can be adjusted to the required values after diode mounting in IC.

The project realization was proceeding in accordance with the work plan.

7 References

[1] I.E. Field. *The Properties of Diamond*, Academic Press, New York, 1992.

[2] M.M. Nazare, A.J. Neves. Properties, Growth and Applications of Diamond, EMIS, Product code: EM026, London, ISBN: 085296785, 2001.

[3] M. Willander, M. Friesel, Omar-ul Wahab, B. Straumal. Silicon carbide and diamond for high temperature device applications, *J. Mat. Sci: Mater. in Electronics* **17**, p.1-25, 2006.

[4] *Physical Properties of Diamond: A Handbook*, Ed. by N.V. Novikov, Naukova Dumka, Kiev, 1987 (in Russian).

[5] V.S. Vavilov, A.A. Gippius, E.A. Konorova. *Electronic and Optical Processes in Diamond*, Nauka, Moscow, 1985 (in Russian).

[6] *Diamond in Electronic Engineering* (*A collection of papers*), Ed. by V.B. Kvaskov, Energoatomizdat, Moscow, 1990 (in Russian).

[7] V.G. Aleshin, A.A. Smekhnov, G.P. Bogatyreva, V.B. Kruk. *Chemistry of Diamond Surface*, Naukova Dumka, Kiev, 1990 (in Russian).

[8] V. Ralchenko, V. Konov. CVD-diamonds: Application in electronics, *Elektronika: Nauka, Tekhnologii, Biznes*, no 4, p.58-67, 2007 (in Russian).

[9] V.G. Ralchenko, A.V. Savel'ev, A.F. Popovich, I.I. Vlasov, S.V. Voronina, E.E. Ashkinazi. Two-layer heat-removing dielectric diamond–aluminum nitride substrates, *Mikroelektronika* **35**(4), p.243-248, 2006 (in Russian).

[10] V. Ralchenko, I. Sychov, I. Vlasov, A. Vlasov, V. Konov, A. Khomich, S. Voronina. Quality of diamond wafers grown by microwave plasma CVD: effects of gas flow rate, *Diamond Relat. Mater.* **8**, p.189-193, 1999.

[11] K.J. Gray, H. Windishmann. Free-standing CVD diamond wafers for thermal management by DC arc jet technology, *Diamond Relat. Mater.* **8**, p.903-908, 1999.

[12] V. Ralchenko, I. Vlasov, V. Frolov, D. Sovyk, A. Karabutov, K. Gogolinsky, V. Yunkin. Nano-and microcrystalline CVD diamond films on surfaces with intricate shape, in A.A. Voevodin et al. (Eds.) *Nanostructured Thin Films and Nanodispersion Strengthened Coatings*, 2004, p.209-220, Kluwer Academic Publishers.

[13] E.V. Ivakin, A.V. Sukhodolov, V.G. Ralchenko, A.V. Vlasov, A.V. Khomich. Measurement of thermal conductivity of polycrystalline CVD diamond using the pulsed dynamic lattices technique. *Kvantovaya Elektronika* **32**(4), p.367-372, 2002 (in Russian).

[14] V.M. Garin, A.N. Kopnin, V.V. Parshin, V.G. Ralchenko, E.E. Chigryai, V.I. Konov, A.B. Mazur, M.P. Parkhomenko. On the mm-wave losses in diamond, *Pis'ma v ZhTF* **25**(7-8), p.85-89, 1999 (in Russian).

[15] V.G. Ralchenko, A.V. Savel'ev, A.F. Popovich, I.I. Vlasov, S.V. Voronina, E.E. Ashkinazi. Two-layer heat-removing dielectric diamond–aluminum nitride substrates. *Mikroelektronika* **35**(4), p.243, 2006 (in Russian).

[16] H.A. Wheeler. Transmission-line properties of a strip on a dielectric sheet on a plane, *IEEE Transactions on Microwave Theory & Techniques* **25**(8), p.631-647, 1977.

[17] V.F. Fusco. *Microwave Circuits. Analysis and Computer-aided Design*, Prentice-Hall, 1987.

[18] K.A. Lukin, P.P. Maksimov. Self-oscillation mode in abrupt *p-n* junctions with constant reverse bias. *Radiofizika i Elektronika* vol. 13, no 2, p.232-238, 2008 (in Russian).

[19] N.S. Boltovets, V.V. Basanets, T.I. Golynnaya, V.A. Krivutsa, L.M. Suvorova, K.A. Lychman. Silicon fast-operating unpackaged p-i-n diodes with beam leads. *Tekhnika i Pribory SVCh* no 2, p.34-36, 2008 (in Russian).
[20] A.E. Belyaev, N.S. Boltovets, L.M. Kapitanchuk, V.P. Kladko, R.V. Konakova, Ya.Ya. Kudryk, A.V. Kuchuk, T.V. Korostinskaya, O.S. Lytvyn, V.V. Milenin, P.V. Nevolin, A.B. Ataubaeva. Au–Ti–n^+-Si and Au–Ti–Pd_2Si–n^+-Si ohmic contacts to silicon microwave diodes. *Tekhnika i Pribory SVCh* no 2, c.31-33, 2009 (in Russian).
[21] K.V. Zinoviev, B.A. Bespalova, A.B. Vasiliev. Study of composition of binary silicate films of boron, phosphorus and antimony diffusion sources obtained from solution compositions. *Elektronnaya Tekhnika. Seriya 6. Materialy* no 11, p.36, 1981 (in Russian).
[22] L.G. Maloratsky. Reviewing the basics of microstrip lines, *Microwaves & RF*, March 2000, p.79-88.
[23] O.S. Moryakov. Diamond heat sinks in design of semiconductor devices, *Obzory po Elektronnoi Tekhnike Ser. 2. Poluprovodnikovye Pribory* no 1(857), 1982 (in Russian).
[24] A.T. Batch. Heat sinking solid-state devices with diamonds, *Electron. Pack. and Production* **10**(8), p.39-44, 1970.
[25] V.G. Aleshin, A.G. Gontar', A.A. Smekhov, D.V. Sokolov. Auger electron spectroscopy at the diamond surface, *Poverkhnost'. Fizika, Khimiya, Mekhanika* no 6, p.146-148, 1987 (in Russian).

8 List of Symbols, Abbreviations, and Acronyms

CVD - chemical vapor deposition
HFSS – high frequency simulation software; high frequency structure simulator
HIC – hybrid integrated circuit
IC – integrated circuit
IMPATT - impact avalanche and transit-time
XRD – x-ray diffraction

S_{11} (S_{21}) – reflection (transmission) coefficient
tanδ - dielectric loss tangent
U_{bias} – diode bias voltage
ε - permittivity
λ_0 - wavelength